Proceedings of the 9ICEG
9th International Congress on Environmental Geotechnics
25-28 June, 2023 | Chania, Greece
© Authors: All rights reserved, 2023
https://doi.org/10.53243/ICEG2023-455

Performance-based design of contaminant barriers for sustainable landfilling and site remediation

A. Dominijanni[1]

[1]*Associate Professor, Politecnico di Torino, Torino, Italy, email: andrea.dominijanni@polito.it*

ABSTRACT

A sustainable approach to the design of contaminant barriers should balance the two conflicting needs of maximising the protection of the groundwater quality and minimising the environmental impact related to the construction of the barrier. In front of this challenge, the most helpful technological innovation is represented by geosynthetic products, such as geomembranes and geosynthetic clay liners, which allow reaching performances equivalent to those of mineral barriers while reducing the consumption of natural resources and emission of greenhouse gases. A second crucial innovation is represented by the transition from a prescriptive-based design approach to a performance-based design approach, which provides a quantification of the risk to human health and the environment due to pollutant migration through the barrier system. The performance-based design guarantees to protect the groundwater resource, avoiding recourse to oversized barrier systems, with relevant economic and environmental savings, and, moreover, encourages adopting the most advanced technologies through a comparison of their performances with respect to traditional systems. This paper focuses on the performance-based design of pollutant containment systems, such as landfill bottom liners and cutoff walls. The effectiveness of pollutant containment systems is demonstrated by calculating the pollutant concentration in the groundwater, which is expected to remain less than some prescribed level at a compliance point. The paper describes analytical and numerical solutions to pollutant transport, which allow the pollutant concentration in the groundwater to be calculated under different boundary conditions. Based on the results obtained from these solutions, the role played not only by the hydraulic and diffusive properties of the containment barriers but also by the hydrogeological features of the site (e.g., the groundwater velocity and the mechanical dispersion within the aquifer) is pointed out.

Keywords: landfill, site remediation, sustainability, groundwater, contaminant migration, analytical and numerical modelling

πολλὰ τὰ δεινὰ κοὐδὲν ἀν-
θρώπου δεινότερον πέλει·
τοῦτο καὶ πολιοῦ πέραν
πόντου χειμερίῳ νότῳ
χωρεῖ, περιβρυχίοισιν
περῶν ὑπ᾽ οἴδμασιν, θεῶν
τε τὰν ὑπερτάταν, Γᾶν
ἄφθιτον, ἀκαμάταν ἀποτρύεται,
ἰλλομένων ἀρότρων ἔτος εἰς ἔτος,
ἱππείῳ γένει πολεύων.

κουφονόων τε φῦλον ὀρ-
νίθων ἀμφιβαλὼν ἄγρει
καὶ θηρῶν ἀγρίων ἔθνη
πόντου τ᾽ εἰναλίαν φύσιν
σπείραισι δικτυοκλώστοις,
περιφραδὴς ἀνήρ· κρατεῖ
δὲ μηχαναῖς ἀγραύλου
θηρὸς ὀρεσσιβάτα, λασιαύχενά θ᾽
ἵππον ὑφέλκεται ἀμφὶ λόφον ζυγὸν
οὔρειόν τ᾽ ἀκμῆτα ταῦρον.

Many the wonders but nothing more wondrous than man.
This thing crosses the sea in the winter's storm,
making his path through the roaring waves.
And she, the greatest of gods, the Earth –
deathless she is, and unwearied – he wears her away
as the ploughs go up and down from year to year
and his mules turn up the soil

The tribes of the lighthearted birds he ensnares, and the races
of all the wild beasts and the salty brood of the sea,
with the twisted mesh of his nets, he leads captive, this clever man.
He controls with craft the beasts of the open air,
who roam the hills. The horse with his shaggy mane
he holds and harnesses, yoked about the neck,
and the strong bull of the mountain.

καὶ φθέγμα καὶ ἀνεμόεν
φρόνημα καὶ ἀστυνόμους
ὀργὰς ἐδιδάξατο καὶ δυσαύλων
πάγων ὑπαίθρεια καὶ
δύσομβρα φεύγειν βέλη
παντοπόρος· ἄπορος ἐπ᾽ οὐδὲν ἔρχεται
τὸ μέλλον· Ἅιδα μόνον
φεῦξιν οὐκ ἐπάξεται
νόσων δ᾽ ἀμηχάνων φυγὰς
ξυμπέφρασται.

Speech and thought like the wind
and the feelings that make the town,
he has taught himself, and shelter against the cold,
refuge from rain. Ever resourceful is he.
He faces no future helpless. Only against death
shall he call for aid in vain. But from baffling maladies
has he contrived escape.

σοφόν τι τὸ μηχανόεν
τέχνας ὑπὲρ ἐλπίδ᾽ ἔχων
τοτὲ μὲν κακόν, ἄλλοτ᾽ ἐπ᾽ ἐσθλὸν ἕρπει·
νόμους γεραίρων χθονὸς
θεῶν τ᾽ ἔνορκον δίκαν
ὑψίπολις· ἄπολις ὅτῳ τὸ μὴ καλὸν
ξύνεστι τόλμας χάριν.
μήτ᾽ ἐμοὶ παρέστιος
γένοιτο μήτ᾽ ἴσον φρονῶν
ὃς τάδ᾽ ἔρδει.

Clever beyond all dreams
the inventive craft that he has
which may drive him one time or another to well or ill.
When he honors the laws of the land and the gods' sworn right
high indeed is his city; but stateless the man
who dares to do what is shameful.

332-375, Sophocles, *Antigone*, 442 BC

1 INTRODUCTION

The Chorus from Sophocles' *Antigone* is probably the first and most famous expression of the wonderment and, at the same time, the worriment before man's powers and deeds. Moving from these poetical verses, the German-American philosopher Hans Jonas elaborated on the moral imperative "Act so that the effects of your action are compatible with the permanence of genuine human life" or expressed negatively: "Act so that the effects of your action are not destructive of the future possibility of such life"; or simply: "Do not compromise the conditions for an indefinite continuation of humanity on earth"; or again turned positive: "In your present choices, include the future wholeness of Man among the object of your will". (Jonas, 1979). Jonas' imperative of Responsibility is the ethical background to the concept of sustainability in engineering practice, which is aimed at designing environmentally compatible, economically viable and socially equitable structures, products and systems that meet the needs of the present without compromising the ability of future generations to meet their own needs.

The application of sustainability criteria to the design of contaminant barriers implicates balancing the two conflicting needs of maximising the protection of the groundwater and minimising the environmental impact of the barrier construction. The traditional method to meet the need to protect the groundwater is to increase the thickness and reduce the hydraulic conductivity of the low-permeability mineral layers of the lining system. The consequence is accepting high economic costs, elevated consumption of natural earth materials and a substantial emission of greenhouse gases for the transportation of raw materials and the construction of the lining system. On the other hand, the need to reduce the economic and environmental impact of barrier construction requires often relying on natural attenuation mechanisms which are affected by high uncertainty. The resulting performance estimation for the barrier system in preventing the effects of contaminant migration is characterised by a high variance and a consequent relatively high probability of failure.

The first fundamental innovation to solve this problem has been using geosynthetics in waste containment and site remediation applications. Geosynthetics allow for a reduction in economic and environmental costs while providing highly controlled and predictable performances. Moreover, composite barriers that consist of a geomembrane overlying a low-permeability mineral layer have been shown to guarantee a performance substantially superior to the single components (geomembrane alone or mineral layer alone). Thick layers of compacted clay can be replaced by thin geosynthetic clay liners characterised by low hydraulic conductivity and high osmotic efficiency when permeated with water solutions with a low solute concentration.

A second crucial innovation is represented by the transition from a prescriptive-based design approach to a performance-based design approach, which provides an assessment of the risk to human health and the environment due to pollutant migration through the barrier system. The performance-based design guarantees to protect the groundwater resource, avoiding recourse to oversized lining systems, with relevant economic and environmental savings. The possibility of modelling the contaminant transport through mineral and geosynthetic liners allows for comparing different types of barrier systems and a theoretically-supported quantification of the expected performance.

A performance-based design of a lining system implies a profound change with respect to the traditional prescriptive-based design, which is still nowadays adopted in several worldwide regulations, especially for waste disposal facilities. The benefits of a performance-based design include (Estrin and Rowe, 1995):

- allowing engineers to bring state-of-the-art knowledge to a project, which in turn is expected to encourage both theoretical and practical research investigations and the application of innovative technology in the field;
- putting emphasis on pre-approval design examination rather than on post-construction monitoring;
- stimulating more in-depth scrutiny by regulators and concerned members of the public regarding the adequacy of the proposed design before approval;
- performing an analysis of the interaction of the proposed engineering system with the particular hydrogeologic conditions in which the landfill would be located.

A common performance criterion is that a liner must ensure that the concentrations of pollutants in the groundwater remain less than prescribed threshold levels at a specified compliance point, which is commonly represented by a monitoring well located in the underlying aquifer and downstream from the contaminated site or the landfill. The pollutant threshold concentration in the compliance point is commonly related to a corresponding acceptable risk to human health and the environment through a toxicological model that considers the pollutant properties and the exposure paths (Dominijanni and Manassero, 2021). The contaminant concentration in the groundwater is obtained from a transport analysis, which considers the migration process from the contaminated site or the waste contained in the landfill to the compliance point.

The approach to follow for landfill lining systems is similar to the procedure used for the risk assessment of contaminated sites that was first developed in the US in the late 1980s (US EPA 1989) and subsequently standardised by the ASTM (ASTM 1995; 2000). This procedure is structured in three tiers (Sethi and Di Molfetta, 2019):

- the first tier essentially involves comparing the site contamination with screening concentration values;
- the second tier involves a simplified contaminant transport analysis based on analytical, semi-analytical, or simple numerical solutions, in which part of the input data are derived from on-site investigations while missing information is obtained from validated and up-to-date databases or from the literature;
- the third tier represents a more detailed appraisal of risk, based on sophisticated models that are solved through advanced numerical methods. These models require enough site-specific chemical, physical and biological data to carry out a full experimental system characterisation.

Although the first tier is not amenable to a risk assessment for the design of a landfill lining system, the second and third tiers can be applied profitably to evaluate the impact of pollutants, released from waste, on groundwater quality.

The application of such a risk assessment to the performance-based design of barrier systems for contaminated sites and landfills can therefore be carried out based on a conceptual model that identifies the contaminated soil or the leachate produced by the waste with the source of contamination and a monitoring piezometer (which may be real or virtual), placed downstream of the site or the landfill, with the point of compliance, as shown in Figure 1.

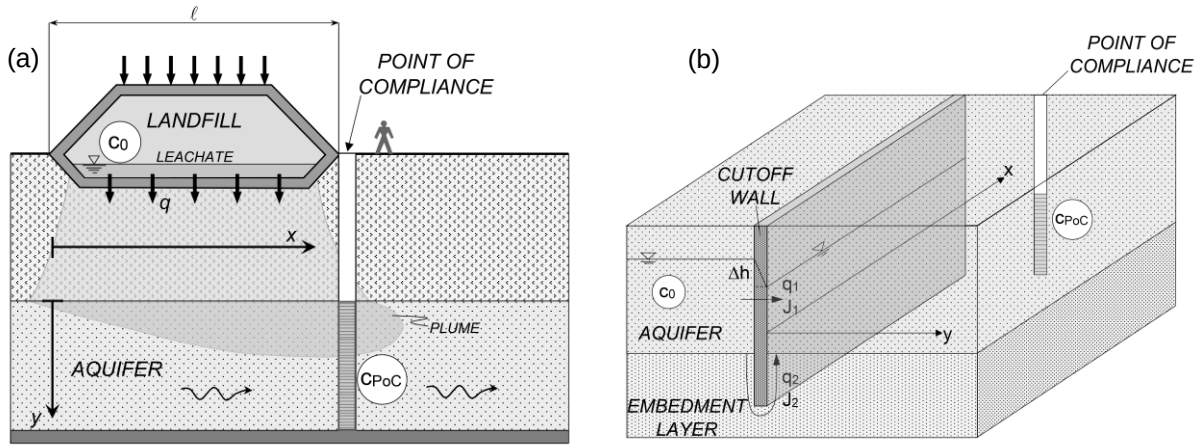


Figure 1. *Reference scheme for the application of the risk assessment procedure to the performed-based design of a barrier system for (a) a landfill and (b) a contaminated site. The contaminant concentration is c_0 in the source (waste leachate or contaminated soil) and c_{PoC} in the point of compliance (typically a monitoring well placed downstream of the landfill or the contaminated site).*

The limit value that the pollutant concentration in the groundwater can assume, in correspondence to the point of compliance, without producing an unacceptable risk to human health or the ecosystem may be determined on the basis of a toxicological model. As a result, the verification of the effectiveness of the barriers system, which may include natural soil layers, in containing the waste contaminations is obtained through a contaminant transport analysis, which provides the theoretical value of the contaminant concentration at the point of compliance. A value of the calculated concentration that is lower than the limit value given by the toxicological model is indicative of a satisfactory design, as the related risk is acceptable.

Dominijanni and Manassero (2021) developed a numerical finite-difference solution to evaluate the contaminant concentration in a confined aquifer beneath a landfill under the restrictive assumptions of steady-state conditions and a constant source concentration in the waste leachate. Analytical solutions were also provided for the specific cases of thin aquifers and infinitely thick aquifers. An analytical solution for the calculation of the leakage rate through a composite liner, which consists of a geomembrane overlying a geosynthetic clay liner, is presented in Guarena et al. (2020) for the case of a hole located in correspondence to a wrinkle in the geomembrane. This solution, which can be implemented in a contaminant migration analysis, considers the influence of bentonite swelling on the determination of the hydraulic transmissivity at the interface between the geomembrane and the underlying geosynthetic clay liner and the chemico-osmotic component of the water flow that is generated by the gradient in the solute concentration. Dominijanni et al. (2021a) have extended the available solutions to scenarios that involve unconfined flow conditions beneath a landfill and a vertical barrier (e.g., a cutoff wall) to prevent lateral migration towards the groundwater flow. These solutions offer the possibility of conducting an analysis that involves a limited number of parameters and allows the influence of the liner properties (e.g., hydraulic conductivity, thickness, defects) and the field conditions (e.g., aquifer thickness, groundwater velocity) on the final result to be appreciated under conservative assumptions (steady-state conditions and constant source concentration). However, these conditions exclude the possibility of modelling time-varying properties and time-dependent phenomena and typically result in conservative predictions of the groundwater contaminant concentration (Shackelford, 1990; Rabideau and Khandelwal, 1998; Rowe et al., 2004). As a result, such solutions should not be considered reliable predictions of the contaminant concentration expected in the aquifer in the long term but conservative estimates of the risk due to contaminant migration and classified as tier 2 analyses for contaminated sites.

Semi-analytical solutions implemented in popular software products, such as POLLUTE (Rowe and Booker, 1985a; Rowe et al., 2004, Rowe and Booker, 2005) and MIGRATE (Rowe and Booker, 1985b), are available to evaluate the groundwater contaminant concentration below a landfill, taking into account the time-evolution of the source concentration in the landfill leachate, as well as time-dependent phenomena, such as adsorption, ion exchange and bio-degradation. These numerical solutions can be compared to a tier 3 analysis for a polluted site, which can be conducted when a more reliable evaluation of the contaminant concentration in the groundwater is considered necessary.

The variation of dominant transport mechanisms that takes place between the vertical movement across the bottom lining system and the underlying attenuation layer and the predominantly horizontal movement that occurs within the aquifer represents a difficulty in conducting a contaminant migration analysis in the landfill scenario. Vertical transport, which can develop under unsaturated conditions, is, in fact, characterised by a low velocity and is therefore mainly controlled by molecular diffusion (Shackelford, 2014). On the contrary, horizontal groundwater movement is typically characterised by a velocity that is some orders of magnitude higher, and the related contaminant transport is dominated by advection. Similar considerations can be made for the migration through a low-permeability vertical barrier and the adjacent aquifer. The numerical methods that are suitable for diffusion-dominated transport may be unsuitable for solving the transport in the aquifer, and this may implicate a loss of accuracy in the calculation. A possible solution to this problem is to resort to the Domain Decomposition Method (Bellomo and Preziosi, 1995). In this method, the domain of the considered mathematical problem is partitioned into sub-domains, which can be analysed separately by introducing additional interface conditions at the boundaries between them. One of the main advantages of the method is the possibility of running a parallel calculation for the different sub-domains. In the scenario of contaminant migration from a landfill, the domain can be divided into a first sub-domain that includes the landfill lining system and the underlying attenuation layer, and a second sub-domain for the aquifer. The interface between the two sub-domains is represented by the top surface of the aquifer, in correspondence to which the continuity of the hydraulic head, the volumetric flux, the contaminant concentration, and the contaminant mass flux have to be imposed. By using such a strategy, it is possible to optimise the choice of the numerical method, as each sub-domain can be solved separately, while an iterative procedure is implemented to check that the interface conditions are satisfied. For instance, a value of the hydraulic head and the contaminant concentrations, at the top of the aquifer, can be assumed at the beginning of the iterative procedure. The vertical volumetric flux and the vertical contaminant flux exiting from the attenuation layer are calculated on the basis of these values. By using these fluxes to impose the boundary conditions at the top of the aquifer sub-domain, a distribution of the hydraulic head and contaminant concentration is found for the groundwater, so that a new estimate of the hydraulic head and the contaminant concentration at the top of the aquifer can be derived. The iterative procedure is stopped when the values of the hydraulic head and the contaminant concentration at the top of the aquifer do not change appreciably between two consecutive calculation steps.

Another possible interesting development of the contaminant migration analysis is its application in the frame of a probabilistic approach in which the boundary conditions and the model parameters have a random nature. In fact, a significant difficulty in the analysis arises from the uncertainty that is encountered in the evaluation of the representative values that need to be assigned to various parameters, such as the leachate contaminant concentration, the hydraulic conductivity of the mineral layers and the number, size and location of the geomembrane defects. In a deterministic approach, the designer must trust in his own good judgement to make the most opportune choice of the values that have to be assigned to the parameters but cannot, however, know the combined effect of the variance of the various parameters on the final result of the analysis. The adoption of a probabilistic approach instead allows the random nature of the involved parameters to be considered explicitly. In such a way, the final results may be related not only to the most representative values of the involved parameters but also to their variance.

The resilience of a project can only be guaranteed through the coupling of a contaminant migration analysis with mechanical stability analysis. Mechanical stresses and strains can influence the barrier performances of the components of a lining system. Rowe and Yu (2018), for instance, reviewed the strains that can develop in a geomembrane liner (GML) from gravel above and below it and from down-drag due to the weight of the waste and from subsequent degradation and consolidation of the waste. These strains play a critical role in the long-term performance of a GML. Stability analyses should consider the effects of seismic actions, extreme rainfall events and large variations in groundwater levels. A key feature of a good design is represented by the attention paid to the consequences of mechanical failures on the barrier performance of a lining system.

This paper focuses on the performance-based design of pollutant containment systems, such as landfill bottom liners and cutoff walls. The presented solutions are derived under the restrictive assumptions of steady-state conditions and constant source concentration, similar to the solutions derived by Dominijanni and Manassero (2021) and Dominijanni et al. (2021a). The volumetric flux through low-permeability barrier systems is initially analysed, taking into account unsaturated conditions and the use of composite barriers that consist of a geomembrane overlying a mineral layer. Successively, the

contaminant mass flux through the barrier system is obtained, and the role of the geomembrane in the composite barrier is addressed. Several solutions are presented for confined and unconfined flow conditions in the aquifer, which can be used for the assessment of the risk to human health and the environment at the compliance point. Lastly, a calculation example is described to illustrate the comparison between two different landfill lining systems.

2 VOLUMETRIC FLUX THROUGH LOW-PERMEABILITY BARRIERS

2.1 Mineral barriers

Under steady-state conditions, the vertical volumetric flux, q, through a landfill lining system that consists of several mineral layers is given by Darcy's law (Harr, 1962; Bear, 1972; Manassero et al., 2000; Rowe et al., 2004):

$$q = k_{eq} \frac{h_p + L - h_b}{L} \tag{1}$$

where k_{eq} is the equivalent hydraulic conductivity, h_p is the height of the ponded leachate above the barrier, L is the total thickness of the barrier system and h_b is the height of the water level at the bottom of the barrier (Figure 2).

The equivalent hydraulic conductivity, k_{eq}, in equation (1) is calculated as the harmonic mean of the hydraulic conductivities of individual layers:

$$k_{eq} = \frac{L}{\sum_{i=1}^{N_l} \frac{L_i}{k_i}} \tag{2}$$

where L_i is the thickness of the i-th layer, k_i is the hydraulic conductivity of the i-th layer and N_l is the number of mineral layers in the barrier system. The calculation of k_{eq} also includes the contribution of natural foundation or attenuation layers (also called geological barriers) that are placed between the artificial barrier system and the underlying aquifer.

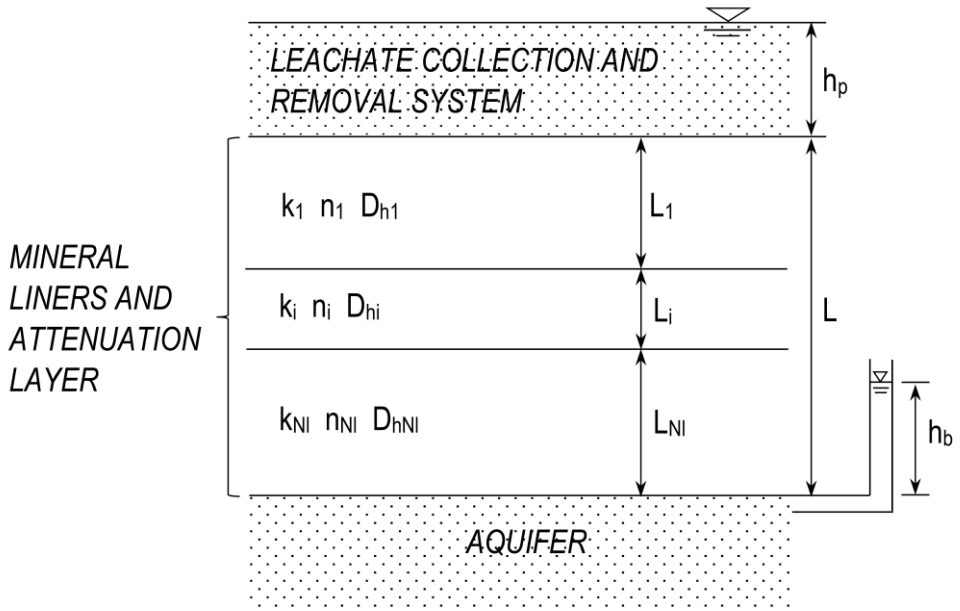


Figure 2. *Vertical profile of a barrier constituted by engineered and/or natural layers.*

The validity of equation (1) is limited to saturated flow conditions with positive hydraulic pressure values. However, these conditions may not occur in the case of a layer with low hydraulic conductivity (layer 1) placed above a layer with higher hydraulic conductivity (layer 2), as pointed out by Giroud et al. (1997). In this case, if the difference in hydraulic conductivity between the two layers is significant, negative values of hydraulic pressure can be reached in the underlying more permeable layer. In order to maintain positive values of hydraulic pressure, the following condition must be fulfilled:

$$k_2\left(1+\frac{h_b}{L_2}\right) \le k_1\left(1+\frac{h_p}{L_1}\right) \tag{3}$$

where k_1 and L_1 represent the hydraulic conductivity and the thickness of the first upper layer, respectively, and k_2 and L_2 represent the hydraulic conductivity and the thickness of the second underlying layer, respectively.

If the condition given by equation (3) is not fulfilled, the volumetric flux through the second layer, q_2, depends on the unsaturated hydraulic conductivity, k_{2uns}, which can be expressed as follows (Gardner, 1958; Philip, 1968; Raats, 1970; Lu and Griffiths, 2004):

$$k_{2uns} = k_2 \cdot \exp(-\alpha_c \cdot \psi) \tag{4}$$

where α_c is an empirical parameter, which depends on the soil pore size and is inversely proportional to the height of the capillary rise and ψ is the soil suction head.

From the integration of the water balance equation, the volumetric flux q_2 is found to be given by (Lu and Griffiths, 2004; Lu and Likos, 2004):

$$q_2 = k_2 \frac{\exp(-\alpha_c \cdot \psi_s) - \exp(-\alpha_c \cdot L_2)}{1-\exp(-\alpha_c \cdot L_2)} \tag{5}$$

where ψ_s is the soil suction head at the interface between the two layers.

At the same time, the volumetric flux through the first upper layer, q_1, can be approximated as follows under saturated conditions:

$$q_1 = k_1 \frac{h_p + L_1 + \psi_s}{L_1}. \tag{6}$$

By imposing the continuity condition between the two fluxes, $q = q_1 = q_2$, the following nonlinear equation is obtained for the suction head at the interface between the two layers:

$$\psi_s = -\frac{1}{\alpha_c} \cdot \ln\left[e^{-\alpha_c \cdot L_2} + \frac{k_1}{k_2}(1-e^{-\alpha_c \cdot L_2})\left(\frac{h_p + L_1}{L_1} + \frac{\psi_s}{L_1}\right)\right]. \tag{7}$$

Two limit conditions can be found by varying the parameter α_c. For high values of α_c, that is, for coarse-grained soils with a negligible ability of water sorption by capillarity, the suction head at the layer interface, ψ_s, tends to zero, and the volumetric flux results to depend only on the hydraulic conductivity of the first layer:

$$q = k_1 \frac{h_p + L_1}{L_1} \tag{8}$$

For low values of α_c, that is, for fine-grained soils with a relevant capillary sorption ability, the volumetric flux tends to the maximum value given by equation (1), which is derived by assuming saturated conditions in all layers.

In the cutoff wall scenario, the volumetric flux consists of two contributions, q_1 and q_2, which represent the horizontal volumetric flux passing through the wall and the vertical volumetric flux passing through the low-permeability soil layer in which the wall is embedded below the aquifer (Figure 1b).

The volumetric flux, q_1, is given by Darcy's equation as follows:

$$q_1 = k_w \frac{\Delta h}{L_w} \tag{9}$$

where Δh is the hydraulic head difference across the cutoff wall and k_w and L_w are the hydraulic conductivity and the thickness of the cutoff wall, respectively.

The volumetric flux, q_2, can be estimated as the one-dimensional flux expressed by the following Darcy's equation:

$$q_2 = k_e \frac{\Delta h}{2d_e} \tag{10}$$

where k_e is the hydraulic conductivity of the low-permeability soil layer underlying the aquifer, and d_e is the embedment depth of the cutoff wall.

2.2 Composite barriers

In the presence of a geomembrane, the evaluation of the volumetric flux through a landfill composite barrier, constituted by a geomembrane and the underlying mineral layers, requires specific treatment. As geomembranes are polymeric sheets that have very low permeability to water (< $1 \cdot 10^{-14}$ m/s), the flow (or leakage) occurs through the holes that are created during the installation of the geomembrane and during any subsequent construction activities, such as the placement of materials on top of the geomembrane (Giroud, 2016). Defects in the geomembrane can range in size from pinholes having a diameter less than the thickness of the geomembrane to defective seams between geomembrane panels that are several meters long (Foose et al., 2001).

Leakage rates for perfect contact conditions between the geomembrane and the underlying mineral barrier can be estimated using a point source solution for the following water mass conservation equations:

$$Q_{2D} = \pi r \cdot \left(-k \frac{dh}{dr} \right) = \text{constant} \quad \text{(plane geometry and integration over a half-circle)} \tag{11}$$

$$Q = 2\pi r^2 \cdot \left(-k \frac{dh}{dr} \right) = \text{constant} \quad \text{(axial-symmetric geometry and integration over a half-sphere)} \tag{12}$$

The following solutions can be found from the integration of equations (11) and (12):

$$h = -\frac{Q_{2D}}{\pi k} \ln(r) + C \quad \text{(plane geometry)} \tag{13}$$

$$h = \frac{Q}{2\pi k} \frac{1}{r} + C \quad \text{(axial-symmetric geometry)} \tag{14}$$

where r is the radial distance from the point source, and C is a constant of integration. The constant C can be obtained by imposing that the hydraulic head is equal to h_b at a radial distance equal to the thickness of the mineral layer, L.

An improvement in the solution can be obtained by introducing an image sink at a specular position with respect to the base of the layer and imposing that $h = h_b$ when $r = r'$, where r' is the radial distance from the image sink (Figure 3).

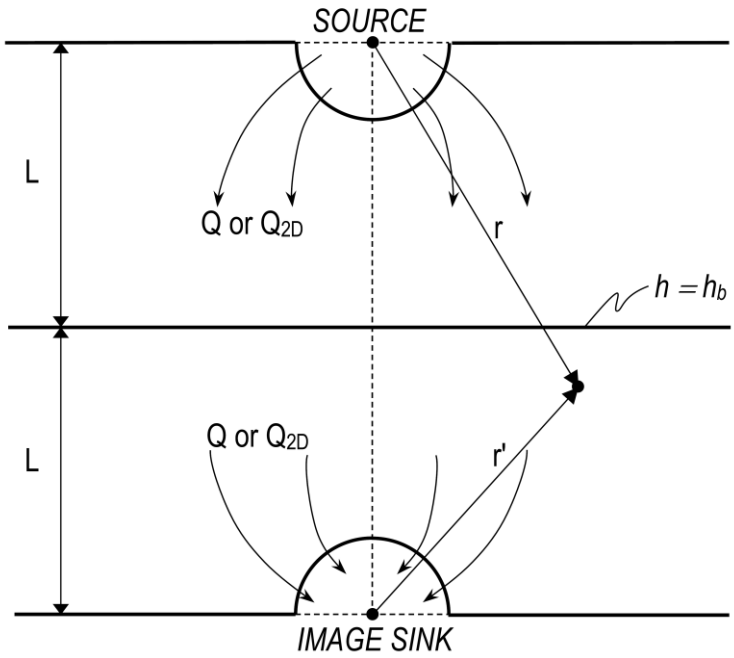


Figure 3. *Reference scheme for the analysis of leakage rate, Q (for axial-symmetric conditions) or Q_{2D} (for plane conditions), through a geomembrane defect using a point source solution with an image sink located specularly at a distance 2L, where L is the thickness of the mineral layer underlying the geomembrane.*

The leakage rate through the defect is obtained by imposing a known hydraulic head in correspondence with the defect boundary. In the case of plane geometry with a defective seam of width 2*b*, the leakage rate is found by imposing that $h = h_p + L$ at $r = b$:

$$Q_{2D} = \pi k \frac{h_p + L - h_b}{\ln\left(\frac{\kappa L}{b}\right)}. \tag{15}$$

where $\kappa = 1$ for the source solution and $\kappa = 2$ for the source-sink solution.

The leakage rate given by equation (15) is referred to an infinitely long defect and is expressed as the volume of water passing through the defect per unit time and unit length. For a rectangular defect of short side 2*b* and long side L_d, the leakage rate can be estimated as follows:

$$Q = Q_{2D} L_d . \tag{16}$$

For an axial-symmetric geometry with a circular hole of radius r_0, the leakage rate is found by imposing that $h = h_p + L$ at $r = r_0$:

$$Q = 2\pi k r_0 \frac{h_p + L - h_b}{\left(1 - \frac{r_0}{\kappa L}\right)}. \tag{17}$$

where $\kappa = 1$ for the source solution and $\kappa = 2$ for the source-sink solution, analogously to plane geometry.

When $h_b = L$ and $L \to \infty$, the latter equation can be compared with the exact Forchheimer's (1930) solution for a circular hole on a semi-infinite isotropic medium ($Q = 4kr_0h_p$). The leakage rate given by equation (17) is found to overestimate the exact solution of a factor $\pi/2$. As a result, the point source solution can be considered a conservative approximate solution.

In many practical applications, the contact between the geomembrane and the underlying soil is not perfect, and a lateral flow is permitted along their interface (Giroud and Bonaparte, 1989; Rowe, 1998). Under such conditions, the quality of the contact between the two components of the composite liner (i.e., the geomembrane and the underlying soil) is one of the key factors that govern the rate of leakage through the composite liner. A theoretical model can be formulated by assuming a lateral flow along the interface between the geomembrane and the underlying soil, and a one-dimensional vertical flow through the mineral barrier underlying the geomembrane. The interface flow rate can be written as follows:

$$Q_{r\,2D} = -\vartheta \frac{dh}{dr} \qquad \text{(plane geometry)} \tag{18}$$

$$Q_r = -2\pi r \vartheta \frac{dh}{dr} \qquad \text{(axial-symmetric geometry)} \tag{19}$$

where ϑ is the interface transmissivity.

The vertical one-dimensional flow is expressed through the following Darcy's equation:

$$q_s = k \frac{h - h_b}{L} \tag{20}$$

where h is a function of the distance, r, from the geomembrane defect.

The mass conservation balance of water in the interface can be written as follows:

$$dQ_{r\,2D} = -q_s dr \qquad \text{(plane geometry)} \tag{21}$$

$$dQ_r = -q_s (2\pi r \cdot dr) \qquad \text{(axial-symmetric geometry)} \tag{22}$$

From these balances, the following equations for the hydraulic head can be derived:

$$\frac{d^2h}{dr^2} - \alpha^2 h = -\alpha^2 h_b \qquad \text{(plane geometry)} \tag{23}$$

$$\frac{d^2h}{dr^2} + \frac{1}{r}\frac{dh}{dr} - \alpha^2 h = -\alpha^2 h_b \qquad \text{(axial-symmetric geometry)} \tag{24}$$

where

$$\alpha = \sqrt{\frac{k}{L \cdot \vartheta}}\,. \tag{25}$$

In the case of plane geometry, the following solution of equation (23) is found by imposing that $h = h_p + L$ at $r = b$ and $h \to h_b$ when $r \to \infty$.

$$h = \begin{cases} h_p + L & \text{if } r < b \\ (h_p + L - h_b)e^{-\alpha(r-b)} + h_b & \text{if } r \geq b \end{cases} \tag{26}$$

The leakage rate through the defective seam is obtained through the following integration:

$$Q_{2D} = 2bk \frac{h_p + L - h_b}{L} + 2 \int_{r=b}^{r\to\infty} k \frac{h - h_b}{L} dr = 2bk \frac{h_p + L - h_b}{L} \left(1 + \frac{1}{\alpha b}\right). \tag{27}$$

The latter equation corresponds to the solution given by Rowe (1998) for the leakage rate through a single hole that coincides with a geomembrane wrinkle when there is no interaction between adjacent wrinkles.

In the case of an axial-symmetric geometry, a similar solution is obtained by imposing that $h = h_p + L$ at $r = r_0$ and $h \to h_b$ when $r \to \infty$.

$$h = \begin{cases} h_p + L & \text{if } r < r_0 \\ (h_p + L - h_b)\dfrac{K_0(\alpha r)}{K_0(\alpha r_0)} + h_b & \text{if } r \geq r_0 \end{cases} \tag{28}$$

The leakage rate through a circular hole is obtained through the following integration:

$$Q = \pi r_0^2 k \frac{h_p + L - h_b}{L} + 2\pi \int_{r=r_0}^{r\to\infty} k \frac{h - h_b}{L} r dr = \pi r_0^2 k \frac{h_p + L - h_b}{L}\left[1 + \frac{2}{r_0 \alpha}\frac{K_1(\alpha r_0)}{K_0(\alpha r_0)}\right]. \tag{29}$$

An empirical equation for the calculation of the leakage rate through a circular hole in a geomembrane with imperfect contact was provided by Giroud (1997):

$$Q = C_q \cdot a_h^{0.1} \cdot h_p^{0.9} \cdot k^{0.74} \cdot \left[1 + 0.1\left(\frac{h_p}{L}\right)^{0.95}\right] \tag{30}$$

where C_q is a dimensionless quality coefficient of the contact between the geomembrane and the underlying mineral layer, which can be assumed equal to 0.21 for good contact conditions and 1.15 for poor contact conditions, and a_h is the circular hole area.

The volumetric flux of water passing through several defects of different sizes and shapes can be expressed as follows:

$$q_d = \sum_{i=0}^{N} n_i Q_i \tag{31}$$

where N is the number of defect types and n_i is the number of defects of the i-th type per unit area (i.e., the frequency of the i-th defect type).

Italian guidelines (ISPRA, 2011) suggest the following formula:

$$q_d = n_{micro-holes} Q_{micro-holes} + n_{holes} Q_{holes} + n_{tears} Q_{tears} \tag{32}$$

where the leakage rates are calculated through equation (30) and the defect frequency and areas are obtained from Table 1.

The equivalent area of a defect, A_e, is defined as the ratio between the leakage rate through the defect and the volumetric flux through the mineral barrier, q, given by equation (1):

$$A_e = \frac{Q}{q}. \tag{33}$$

Table 1. *Distribution of geomembrane defect features (ISPRA, 2011)*

Defect type	**Geomembrane defects**							**Area of geomembrane defects**		
	Probability distribution	Frequency of defects with QC* (number/ha)			Frequency of defects without QC (number/ha)			Probability distribution	Area of defects (m^2)	
Micro-holes	triangular	0	25	25	0	750	750	Log uniform	$1 \cdot 10^{-8}$	$5 \cdot 10^{-6}$
Holes	triangular	0	5	5	0	150	150	Log uniform	$5 \cdot 10^{-6}$	$1 \cdot 10^{-4}$
Tears	triangular	0	0.1	2	0	0.5	10	Log uniform	$1 \cdot 10^{-4}$	$1 \cdot 10^{-2}$

*QC = Quality Control

When multiple defects are taken into account, the fraction, a_d, of the overall equivalent area over the area of the lining system can be expressed as follows:

$$a_d = \sum_{i=1}^{N} n_i A_{ei} = \frac{\sum_{i=1}^{N} n_i Q_i}{q} \tag{34}$$

where n_i is the number of defects of the i-th type per unit area, A_{ei} is the equivalent area of the defects of the i-th type, Q_i is the leakage rate through the defect of the i-th type and q is the volumetric flux through the mineral barrier underlying the geomembrane.

It is worth observing that the leakage rate becomes null when $h_p = 0$ based on Giroud's empirical equation (30), while this does not occur using theoretical solutions unless $h_b = L$. In fact, the theoretical solutions have been derived under the assumption that the soil remains fully saturated when the hydraulic pressure is negative. As a consequence, even in the absence of a leachate head ponded on the barrier (i.e., $h_p = 0$), a vertical volumetric flux takes place with negative water pressure until the hydraulic head at the top of the liner is higher than h_b. For instance, if $h_b = 0$, then the condition of no leakage rate is found when $h_{TOP} = h_p + L = 0$, i.e., when the water pressure at the top of the liner, $u_{TOP} = \gamma_w \cdot (h_{TOP} - L)$ is equal to $-\gamma_w L$. A similar result is also valid for mineral barriers without an overlying geomembrane. As the leachate drainage layer stops collecting water when $h_p = 0$, this result implies that a vertical volumetric flux can occur without water diversion in the leachate drainage layer when specific head conditions are met.

Another observation of interest about Giroud's empirical equation is that it shows a dependency on the mineral layer thickness, L, which is much less relevant than in the theoretical solutions. This result appears to be a consequence of Giroud's assumption that Q is a function of h_p only and not of the hydraulic head difference across the mineral layer given by $h_p + L - h_b$.

In the case of composite slurry cutoff walls, leakage can occur in correspondence with geomembrane joints. On the basis of the previous studies of Dachler (1936), Manassero et al. (1995) derived the following solution, which takes into account the spacing, I, between joints (Figure 4):

$$Q_{2D} = \frac{\frac{\pi k_w \Delta h}{2}}{\frac{\pi S}{2I} + \frac{\pi k_w l_j}{2 k_j d} - \ln\left(\sin\frac{\pi d}{2I}\right)} \tag{35}$$

where k_w is the hydraulic conductivity of the slurry wall without the geomembrane, S is the thickness of the wall, I is the joint spacing, l_j is the length of the joint path, k_j is the equivalent hydraulic conductivity of the path internal to the joint and d is the equivalent joint opening.

A similar solution can be found using the point source-sink solution for a plane geometry given by equation (15) with $\kappa = 2$, if the interaction between adjacent joints is neglected:

$$Q_{2D} = \frac{\frac{\pi k_w \Delta h}{2}}{\ln\left(\frac{2S}{d}\right) + \frac{\pi k_w l_j}{2 k_j d}} . \tag{36}$$

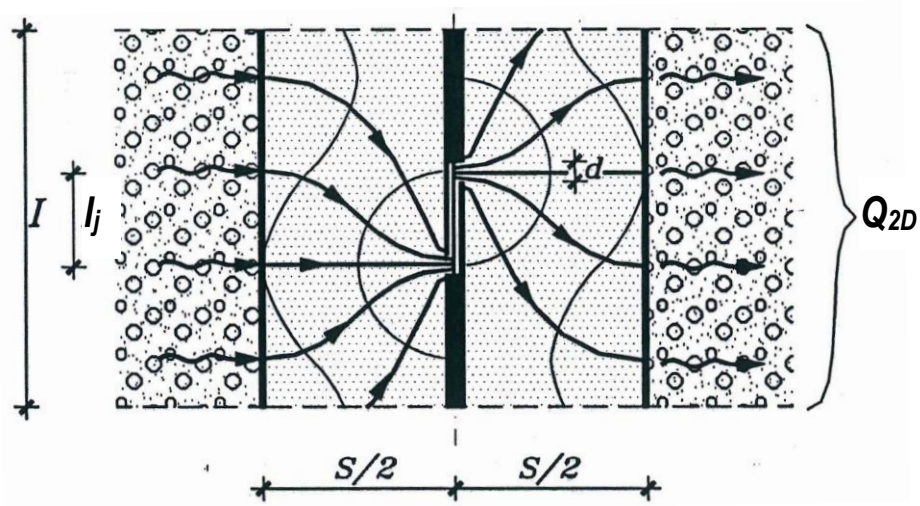


Figure 4. *Reference scheme for the analysis of leakage rate, Q_{2D}, through joints of a geomembrane placed in a cutoff slurry wall.*

3 CONTAMINANT FLUX THROUGH LOW-PERMEABILITY BARRIERS

3.1 Mineral barriers

Under steady-state conditions, the vertical flux of a miscible contaminant through a saturated multi-layer mineral barrier is given by (Dominijanni et al., 2021b):

$$j_{ss}^{ad} = n_{e,s} \frac{q}{n_{e,w}} \frac{c_0 \cdot e^{P_L} - c_x}{e^{P_L} - 1} \tag{37}$$

where $n_{e,w}$ is the water-effective porosity, which does not include the inaccessible or occluded pores, $n_{e,s}$ is the solute-effective porosity, which can be lower than $n_{e,w}$ due to solute charge repulsion or steric hindrance mechanisms, q is the volumetric flux given by equation (1), c_0 is the pollutant concentration in the leachate on the top of the barrier, c_x is the pollutant concentration at the bottom of the barrier, which is supposed to coincide with the top of the aquifer located below the landfill, and P_L is the dimensionless Peclet number of the mineral barrier.
The Peclet number, which represents the ratio of the advective transport rate to the diffusive-dispersive transport rate, can be expressed as follows (Dominijanni et al., 2021b):

$$P_L = \frac{q}{\Lambda} \tag{38}$$

where Λ is the equivalent diffusivity of the multi-layer mineral barrier, which is given by:

$$\Lambda = \frac{1}{\int_0^L \frac{dz}{\vartheta_{e,w} \cdot D_h}} \tag{39}$$

where $\vartheta_{e,w}$ is the volumetric content accessible to mobile water, D_h is the contaminant hydrodynamic dispersion coefficient, and z is the distance from the top of the barrier.

For the sake of simplicity, in the remaining part of this paper, the presence of occluded pores and the mechanisms of solute charge-repulsion and steric hindrance are neglected, and therefore the water-effective porosity is assumed to coincide with the solute-effective porosity and the total porosity, n.
When the contaminant transport occurs under saturated conditions through a multi-layer system, in which n_i and D_{hi} are the porosity and the hydrodynamic dispersion coefficient of the i-th layer, respectively, Λ can be expressed as follows:

$$\Lambda = \frac{1}{\sum_{i=1}^{N_l} \frac{L_i}{n_i D_{hi}}} \tag{40}$$

where L_i is the length of the i-th layer and N_l is the number of mineral layers.

The coefficient D_{hi} is determined as the sum of two contributions, that is, the mechanical dispersion coefficient, D_{mi}, which accounts for the mixing or spreading of the solute front during migration due to variations in the seepage velocity, and the effective diffusion coefficient, D^*_i, which accounts for mixing or spreading of the solute due to molecular diffusion:

$$D_{hi} = D_{mi} + D_i^* . \tag{41}$$

The mechanical dispersion coefficient is typically expressed as a linear function of the seepage velocity, $v_i = \frac{q}{n_i}$, in the following way (Bear, 1972; Shackelford, 1993; Rowe et al., 2004):

$$D_{mi} = \alpha_i v_i \tag{42}$$

where α_i is the longitudinal dispersivity, which, in the absence of data obtained from the laboratory or in situ tests, can be preliminarily assumed equal to 10% of the thickness of the barrier layer, $\alpha \approx 0.1 \cdot L$ (Shackelford and Rowe 1998, Guyonnet et al. 2001). More advanced models based on a random representation of hydraulic conductivity may be used to simulate the mechanical dispersion phenomenon without resorting to a mechanical dispersion coefficient (Dominijanni et al., 2021b).

The effective diffusion coefficient can be expressed as a function of the free solution diffusion coefficient of solute, D_0, as follows (Shackelford and Daniel, 1991a; Shackelford, 2014):

$$D_i^* = \tau_{mi} D_0 \tag{43}$$

where τ_{mi} is the matrix tortuosity factor, which falls within the $0 \leq \tau_{mi} \leq 1$ range. When the seepage velocity tends to zero, the contribution of mechanical dispersion becomes negligible, and it is, therefore, possible to assume $D_{hi} \approx D^*_i$ as a first approximation.

3.2 Composite barriers

If the barrier includes a geomembrane, a distinction has to be made between inorganic chemicals, whose diffusion through geomembranes is extremely slow and can be neglected with respect to transport through geomembrane holes, and organic compounds, such as VOC, which can partition into the polymer and diffuse relatively rapidly, due to the limited geomembrane thickness (Rowe, 1998; Shackelford, 2014).

A decomposition of the contaminant flux into two components can be made to model the transport of contaminants through composite barriers using a one-dimensional approach. The first flux component, of relevance for both inorganic contaminants and volatile organic compounds (VOCs), is represented by the flux through the geomembrane defects, which is assumed to be expressed as a one-dimensional flux through an equivalent area. The second flux component, of interest only for VOCs, is represented by the diffusive flux through the geomembrane, which is hypothesised to occur over the remaining part of the total area.

The steady-state advective-dispersive flow rate for perfect contact conditions between the geomembrane and the underlying mineral barrier can be estimated using a point source solution for the following contaminant mass conservation equations:

$$J_{ss2D} = Q_{2D} c - \pi r \cdot n D_h \frac{dc}{dr} = \text{ constant} \qquad \text{(plane geometry and integration over a half-circle)} \tag{44}$$

$$J_{ss} = Qc - 2\pi r^2 \cdot nD_h \frac{dc}{dr} = \text{constant (axial-symmetric geometry and integration over a half-sphere)} \quad (45)$$

The integration of equations (44) and (45) can be carried out by imposing the condition $c = c_b$ at a radial distance, r, equal to the thickness of the mineral layer, L.

In the case of plane geometry, the resulting contaminant flow rate is found by assuming that $c = c_0$ at $r = b$:

$$J_{ss2D} = Q_{2D} \frac{c_0 \left(\frac{L}{b}\right)^{\frac{Q_{2D}}{\pi n D_h}} - c_b}{\left(\frac{L}{b}\right)^{\frac{Q_{2D}}{\pi n D_h}} - 1}. \quad (46)$$

where Q_{2D} is given by equation (15) with $\kappa = 1$.

The equivalent area for the contaminant flow rate is defined as follows:

$$J_{ss2D} = A_{e2D}^s q \frac{c_0 e^{P_L} - c_b}{e^{P_L} - 1} \quad (47)$$

and results to coincide with the equivalent area, $A_{e2D} = \dfrac{Q_{2D}}{k \dfrac{h_p + L - h_b}{L}}$, for the leakage flow rate:

$$A_{e2D}^s = A_{e2D} = \frac{\pi L}{\ln\left(\frac{L}{b}\right)}. \quad (48)$$

In the case of an axial-symmetric geometry, the contaminant flow rate is obtained by imposing that $c = c_0$ at $r = r_0$:

$$J_s = Q \frac{c_0 e^{\frac{Q}{2\pi r_0 n D_h}\left(1 - \frac{r_0}{L}\right)} - c_b}{e^{\frac{Q}{2\pi r_0 n D_h}\left(1 - \frac{r_0}{L}\right)} - 1}. \quad (49)$$

where Q is given by equation (17) with $\kappa = 1$.

For the axial-symmetric geometry, the equivalent area for the contaminant flux is defined as follows:

$$J_{ss} = A_e^s q \frac{c_0 e^{P_L} - c_b}{e^{P_L} - 1} \quad (50)$$

and results to coincide with the equivalent area, $A_e = \dfrac{Q}{k \dfrac{h_p + L - h_b}{L}}$, for the leakage flow rate:

$$A_e^s = A_e = \frac{2\pi r_0 L}{\left(1 - \frac{r_0}{L}\right)}. \quad (51)$$

As a consequence of this analysis, the equivalent area for the contaminant flow rate can be taken equal to the equivalent area evaluated for the volumetric leakage flow rate, at least for the case of a point-source solution.

An additional evaluation can be carried out by taking into account the horizontal flow in the interface between the geomembrane and the underlying mineral layer. In this case, the following mass conservation equations may be derived neglecting diffusive transport through the interface:

$$d\left(Q_{r\,2D}c\right) = -q_s \frac{ce^{\frac{q_s L}{nD_h}} - c_b}{e^{\frac{q_s L}{nD_h}} - 1} dr \qquad \text{(plane geometry)} \qquad (52)$$

$$d\left(Q_r c\right) = -q_s \frac{ce^{\frac{q_s L}{nD_h}} - c_b}{e^{\frac{q_s L}{nD_h}} - 1} (2\pi r \cdot dr) \qquad \text{(axial-symmetric geometry)} \qquad (53)$$

where q_s is given by equation (20), and h is given by equation (26) for a plane geometry and equation (28) for an axial-symmetric geometry.

These equations can be integrated to find the concentration c in the interface. The resulting vertical flux is obtained by the following integrals:

$$J_{ss2D} = 2b \cdot q \frac{c_0 e^{P_L} - c_b}{e^{P_L} - 1} + 2 \cdot \int_b^\infty \left(k \frac{h - h_b}{L} \right) \left[\frac{c \cdot e^{\frac{k(h-h_b)}{nD_h}} - c_b}{e^{\frac{k(h-h_b)}{nD_h}} - 1} \right] dr \qquad \text{(plane geometry)} \qquad (54)$$

$$J_{ss} = \pi r_0^2 \cdot q \frac{c_0 e^{P_L} - c_b}{e^{P_L} - 1} + 2\pi \cdot \int_{r_0}^\infty \left(k \frac{h - h_b}{L} \right) \left[\frac{c \cdot e^{\frac{k(h-h_b)}{nD_h}} - c_b}{e^{\frac{k(h-h_b)}{nD_h}} - 1} \right] r dr \qquad \text{(axial-symmetric geometry)} \qquad (55)$$

Calculation of the contaminant flow rate requires a numerical solution. However, the equivalent area that is obtained from this analysis is logically expected to be lower than the equivalent area found for the volumetric leakage flow rate, as the contribution of the diffusive transport through the soil liner determines an increase in the rate of concentration decay in the interface with respect to the case of pure advection.

Based on such consideration, a_d, as defined in equation (34), is a conservative estimate of the fraction of the barrier total area which undergoes a one-dimensional contaminant flux equivalent to the contaminant flux through the geomembrane defects.

The diffusive flux of organic contaminant (VOCs), which occurs over the fraction (1 – a_d) of the total area, is given by:

$$j_{ss}^d = \Lambda_d (c_0 - c_x) \qquad (56)$$

where

$$\Lambda_d = \frac{1}{\frac{L_g}{K_g D_g} + \frac{1}{\Lambda}} \qquad (57)$$

where L_g is the thickness of the geomembrane, K_g is the partition coefficient between the geomembrane and solute, and D_g is the diffusion coefficient of the geomembrane. Values of K_g and D_g for several organic contaminants are provided by Rowe et al. (2004). The diffusion coefficient D_g for inorganic compounds is generally negligible and can be assumed to be null for practical purposes.

The total flux that takes place through the composite barrier is given by:

$$j_{ss} = a_d j_{ss}^{ad} + (1-a_d) j_{ss}^{d} = a_d q \frac{c_0 e^{P_L} - c_x}{e^{P_L} - 1} + (1-a_d)\Lambda_d (c_0 - c_x) \tag{58}$$

The following special cases can be pointed out:

a) in case of an intact geomembrane (i.e., in the absence of geomembrane defects), $a_d = 0$ and, as a result, the contaminant flux is purely diffusive;
b) in case of a degraded geomembrane, which has lost its efficiency, it can be assumed $a_d = 1$, so that the contaminant flux results to be entirely advective-diffusive;
c) when $P_L > 4$, the advective component of contaminant transport is predominant over the diffusive one and equation (58) becomes

$$j_{ss} = a_d q c_0 + (1-a_d)\Lambda_d (c_0 - c_x)\,. \tag{59}$$

In the cutoff wall scenario, a similar equation for the contaminant flux can be derived, considering the different possible paths of migration:

$$j_{ss} = a_{d1} q_1 \frac{c_0 e^{P_{L1}} - c_x}{e^{P_{L1}} - 1} + (1-a_{d1})\Lambda_{d1}(c_0 - c_x) + q_2 \frac{c_0 e^{P_{L2}} - c_x}{e^{P_{L2}} - 1} \tag{60}$$

where c_x is the contaminant concentration at the boundary between the wall and the aquifer, q_1 and q_2 are given by equations (9) and (10), respectively, and the other parameters are defined as follows:

$$a_{d1} = n_j \frac{\frac{\pi L_w}{2}}{\ln\left(\frac{2L_w}{d}\right) + \frac{\pi k l_j}{2k_j d}} \tag{61}$$

$$P_{L1} = \frac{q_1 L_w}{n_w D_{hw}} \tag{62}$$

$$\Lambda_{d1} = \frac{1}{\frac{L_g}{K_g D_g} + \frac{L_w}{n_w D_{hw}}} \tag{63}$$

$$P_{L2} = \frac{q_2 d_e}{n_e D_{he}} \tag{64}$$

where n_j is the number of geomembrane joints per unit length, $L_w = S$ is the thickness of the cutoff wall, n_w and D_{hw} are the porosity and the hydrodynamic dispersion coefficient of the cutoff wall, respectively, and n_e and D_{he} are the porosity and the hydrodynamic dispersion coefficient of the embedment layer, respectively (Figure 5).

The contaminant flux equation (60) can also be used in the case of a wall without the geomembrane by assuming $a_d = 1$.

4 CONTAMINANT CONCENTRATION IN THE AQUIFER

The pollutant mass balance within a non-deformable aquifer beneath a landfill can be expressed as follows (Figure 6):

$$n_{aq}\frac{\partial c}{\partial t} = n_{aq}\frac{\partial}{\partial x}\left(D_{h,x}\frac{\partial c}{\partial x}\right) + n_{aq}\frac{\partial}{\partial y}\left(D_{h,y}\frac{\partial c}{\partial y}\right) - \frac{\partial}{\partial x}\left(q_x c\right) - \frac{\partial}{\partial y}\left(q_y c\right) \tag{65}$$

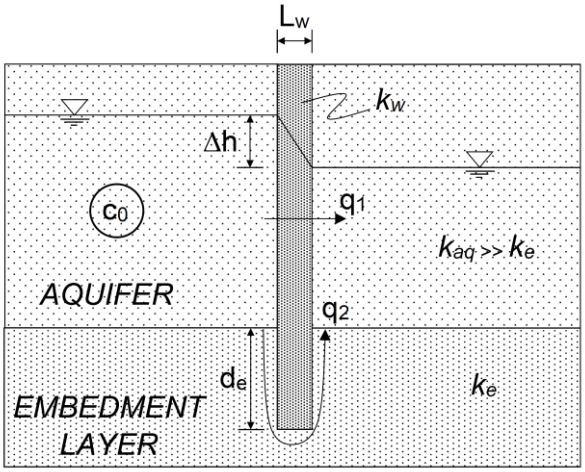


Figure 5. *Vertical section of a cutoff wall embedded in a low-permeability layer. L_w = cutoff wall thickness, Δh = loss of hydraulic head across the cutoff wall; d_e = depth of embedment; c_0 = source pollutant concentration, q_1 volumetric flux through the cutoff wall, q_2 = volumetric flux through the embedment layer, k_{aq} = hydraulic conductivity of the aquifer, k_e = hydraulic conductivity of the embedment layer, k_w = hydraulic conductivity of the cutoff wall.*

where n_{aq} is the aquifer porosity, $c = c(x,y)$ is the pollutant concentration within the aquifer, x is the horizontal distance beneath the landfill, y is the vertical distance from the top of the aquifer, $D_{h,x}$ and $D_{h,y}$ are the horizontal and vertical hydrodynamic dispersion coefficients in the aquifer, respectively, and q_x and q_y are the horizontal and vertical components of the groundwater volumetric flux in the aquifer, respectively.

Under steady-state conditions, and assuming pure advection as the dominant transport mechanism in the horizontal direction, the mass balance is represented by a parabolic partial differential equation (Rubin and Buddemeier, 1996; Charbeneau, 2000):

$$\frac{\partial}{\partial x}\left(q_x c\right) = n_{aq}\frac{\partial}{\partial y}\left(D_{h,y}\frac{\partial c}{\partial y}\right) - \frac{\partial}{\partial y}\left(q_y c\right). \tag{66}$$

Based on the Dupuit-Forchheimer approximation, which assumes vertical equipotential lines, the volumetric balance of water in the horizontal direction can be expressed as follows:

$$\frac{dQ_x}{dx} = a_d q \tag{67}$$

where Q_x is the groundwater discharge in the horizontal direction, and $a_d q$ is the vertical volumetric flux exiting from the barrier system of the landfill.

From the integration of the latter equation, the horizontal discharge is found to vary linearly below the landfill:

$$Q_x = Q_{x0} + a_d q x\,. \tag{68}$$

where Q_{x0} is the discharge at the location $x = 0$.

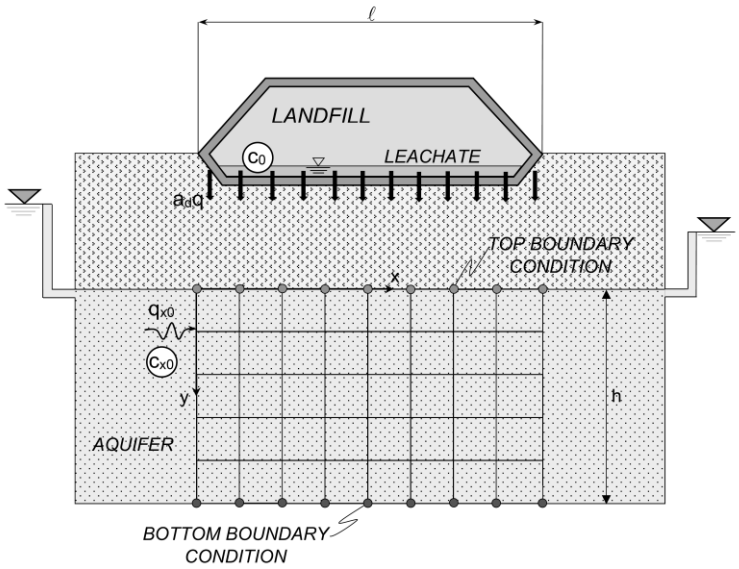


Figure 6. *Reference scheme for the scenario of a confined aquifer beneath a landfill.*

In the case of a confined aquifer of thickness h, the horizontal volumetric flux is given by:

$$q_x = \frac{Q_x}{h} = q_{x0} + \frac{a_d q}{h} x \tag{69}$$

where $q_{x0} = Q_{x0}/h$ is the horizontal volumetric flux at the location $x = 0$.

The vertical groundwater flux, q_y, can be derived from the integration of the following continuity equation:

$$\frac{\partial q_x}{\partial x} + \frac{\partial q_y}{\partial y} = 0 \tag{70}$$

Using equation (69) for q_x and imposing $q_y = 0$ at $y = h$, the following solution is obtained:

$$q_y = a_d q \left(1 - \frac{y}{h}\right). \tag{71}$$

If the horizontal volumetric flux in the aquifer is appreciably greater than the vertical volumetric flux, then the transverse mechanical dispersion can be assumed to be dominant relative to molecular diffusion and the longitudinal mechanical dispersion in the vertical direction (Rubin and Buddemeier, 1996). As a result, the coefficient $D_{h,y}$ can be calculated as follows:

$$D_{h,y} = \alpha_T v_{x0} \tag{72}$$

where α_T is the transverse dispersivity within the aquifer, and $v_{x0} = q_{x0}/n_{aq}$ is the horizontal seepage velocity of groundwater upstream from the landfill.

The pollutant mass balance can be expressed using equations (66), (70) and (72), as follows:

$$q_x \frac{\partial c}{\partial x} = \alpha_T q_{x0} \frac{\partial^2 c}{\partial y^2} - q_y \frac{\partial c}{\partial y} . \tag{73}$$

The boundary condition associated with equation (73) at the top of the aquifer (i.e., at $y = 0$) is obtained by imposing continuity between the vertical solute flux coming from the landfill and the vertical solute flux entering the aquifer:

$$q_y c - \alpha_T q_{x0} \frac{\partial c}{\partial y} = a_d q \frac{c_0 e^{P_L} - c}{e^{P_L} - 1} + (1 - a_d)\Lambda_d (c_0 - c) \quad \text{at } y = 0 . \tag{74}$$

If the bottom of the aquifer is constituted by an impermeable layer, the boundary condition at $y = h$ is given by

$$q_y c - \alpha_T q_{x0} \frac{\partial c}{\partial y} = 0 \quad \text{at } y = h . \tag{75}$$

The following initial condition is then sufficient to formulate the mathematical problem pertaining to the mass balance:

$$c = c_{x0} \quad \text{at } x = 0 . \tag{76}$$

where c_{x0} is the contaminant concentration upstream from the landfill.

A numerical solution to this problem can be obtained by adopting a step-by-step calculation procedure, in which a discretisation based on centred finite differences in direction y and the forward Euler method are used to integrate with respect to variable x. The details of the numerical solution can be found in Dominijanni and Manassero (2021).

Analytical solutions can be derived for the cases of thin aquifers and thick aquifers with $a_d q / q_{x0} < 0.01$. Moreover, the numerical solution can be adapted to solve the case of unconfined flow conditions.

4.1 Thin aquifers

If the thickness of the aquifer, h, is no more than a few meters, the pollutant concentration can be assumed to be invariant with the vertical position. Under steady-state conditions, the pollutant mass balance inside the aquifer can be obtained by combining the horizontal advective mass flux with the vertical mass flux derived from the landfill, j_{ss}, as follows (Figure 7a):

$$\frac{d(Q_x c_x)}{dx} = j_{ss} \tag{77}$$

where j_{ss} is given by equation (58).

The mass balance given by equation (77) can be solved numerically when a_d, q, P_L and Λ_d vary with the distance x, or analytically when all the parameters are constant or are given by piecewise-defined constant functions. The case of landfill with an attenuation layer variable along x is shown in Figure 7b. In a similar case, the total length of the landfill can be split into three parts, in correspondence with which mean values of the parameters can be adopted.

The analytical solution, associated with the boundary condition

$$c_x (x = 0) = c_{x0} \tag{78}$$

where c_{x0} is the initial groundwater contaminant concentration that comes from upstream of the landfill, is given by (Dominijanni and Manassero, 2021; Dominijanni et al., 2021a):

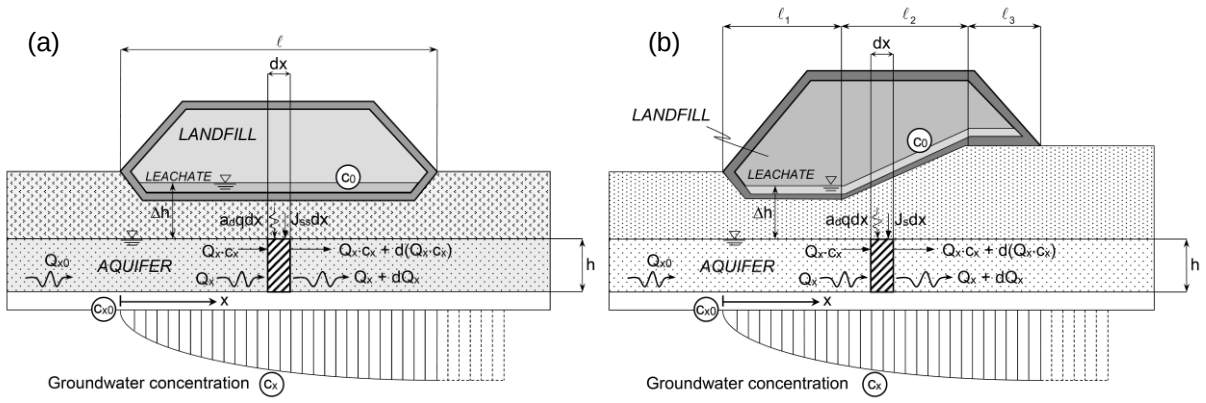


Figure 7. *Reference scheme for the water balance and contaminant mass balance within a thin aquifer beneath the landfill. Constant thickness of the attenuation layer in (a) and variable thickness of the attenuation layer in (b).*

$$RC = 1 - \left(\frac{\eta}{\eta + X} \right)^{\kappa} \tag{79}$$

where

$$RC = \frac{c_x - c_{x0}}{c_0 - c_{x0}} \tag{80}$$

$$X = \frac{x}{\ell} \tag{81}$$

$$\eta = \frac{Q_{x0}}{a_d q \ell} \tag{82}$$

$$\kappa = \frac{e^{P_L}}{e^{P_L} - 1} + \frac{(1 - a_d)\Lambda_d}{a_d q} \tag{83}$$

being ℓ the length of the landfill in the groundwater flow direction.

The following limit conditions can be met:

1) $a_d = 0$, when the geomembrane is perfectly intact (without defects). In such case, equation (79) reduces to:

$$RC = 1 - \exp\left(-\frac{\Lambda_d \ell}{Q_{x0}} X \right) \tag{84}$$

2) $a_d = 1$, when the geomembrane is assumed to be completely degraded. In such case, if $P_L > 4$, $\kappa \to 1$ and equation (79) becomes:

$$RC = 1 - \left(\frac{\eta}{\eta + X} \right). \tag{85}$$

4.2 Semi-infinite aquifers under confined conditions

An analytical solution can be found for cases in which the aquifer thickness is very large by assuming a semi-infinite aquifer and neglecting vertical advection in comparison to vertical transverse mechanical dispersion in the mass balance (but not in the boundary condition at y = 0). Since $h \to \infty$ for a semi-infinite aquifer, the horizontal volumetric flux given by equation (69) can be assumed constant (i.e., $q_x = q_{x0}$) and the mass balance can be expressed as follows:

$$\frac{\partial c}{\partial x} = \alpha_T \frac{\partial^2 c}{\partial y^2}\,. \tag{86}$$

An analytical solution to equation (86), associated with the boundary condition given by equation (74) and the initial condition given by equation (76), can be derived from the set of solutions provided by Carslaw and Jaeger (1959) and Crank (1975) for heat and diffusion problems as follows:

$$RC = erfc\left(\frac{Y}{2\sqrt{X}}\right) - \exp\left(\Gamma Y + \Gamma^2 X\right)\cdot erfc\left(\frac{Y}{2\sqrt{X}} + \Gamma\sqrt{X}\right) \tag{87}$$

where

$$Y = \frac{y}{\sqrt{\alpha_T \ell}} \tag{88}$$

$$\Gamma = \frac{\sqrt{\alpha_T \ell}}{\alpha_T q_{x0}}\left[a_d q \frac{e^{P_L}}{e^{P_L}-1} + (1-a_d)\Lambda_d\right]. \tag{89}$$

4.3 Cutoff wall scenarios

The scenario of a cutoff wall embedded in a low-permeability layer shown in Figure 1b is analogous to the case of a semi-infinite aquifer beneath a landfill (with a rotation of the *y*-axis).

In this scenario, the boundary condition at $y = 0$ becomes:

$$q_y c - \alpha_T q_{x0}\frac{\partial c}{\partial y} = a_{d1} q_1 \frac{c_0 e^{P_{L1}} - c}{e^{P_{L1}}-1} + (1-a_{d1})\Lambda_{d1}(c_0 - c) + q_2 \frac{c_0 e^{P_{L2}} - c}{e^{P_{L2}}-1}\,. \tag{90}$$

where $q_y = a_{d1}q_1 + q_2$.

As a result, when $a_{d1}q_1 + q_2 < 0.01\cdot q_{x0}$, the solution (87) can be adapted to calculate the concentration in the aquifer adjacent to the cutoff wall by assuming the following:

$$\Gamma = \frac{\sqrt{\alpha_T \ell}}{\alpha_T q_{x0}}\left[a_{d1} q_1 \frac{e^{P_{L1}}}{e^{P_{L1}}-1} + (1-a_{d1})\Lambda_{d1} + q_2 \frac{e^{P_{L2}}}{e^{P_{L2}}-1}\right]. \tag{91}$$

4.4 Thick aquifers under confined conditions

The analytical solution for semi-infinite aquifers is sufficiently accurate when the ratio of the aquifer thickness, *h*, to the landfill length, ℓ, is greater than 10% ($h/\ell > 0.1$). If this condition is not fulfilled, an improvement to the analytical solution given by equation (87) can be obtained by reflecting the concentration curve at the bottom impermeable boundary (i.e., at $y = h$) and superimposing the reflected curve onto the original one. Repeating this procedure a number $j = r$ of times, the resulting solution can be expressed as follows:

$$\begin{aligned} RC = \sum_{j=1}^{r} & erfc\left(\frac{2Y_{aq}(j-1)+Y}{2\sqrt{X}}\right) - \exp\left[\Gamma(2Y_{aq}(j-1)+Y) + \Gamma^2 X\right] erfc\left(\frac{2Y_{aq}(j-1)+Y}{2\sqrt{X}} + \Gamma\sqrt{X}\right) + \\ & + erfc\left(\frac{2Y_{aq}j - Y}{2\sqrt{X}}\right) - \exp\left[\Gamma(2Y_{aq}j - Y) + \Gamma^2 X\right] erfc\left(\frac{2Y_{aq}j - Y}{2\sqrt{X}} + \Gamma\sqrt{X}\right) \end{aligned} \tag{92}$$

where $Y_{aq} = h / \sqrt{\alpha_T \ell}$ is the relative depth of the aquifer.

4.5 Thick aquifers under unconfined conditions

When the aquifer beneath the landfill is characterised by unconfined flow conditions, the thickness of the saturated flow, h, varies with the horizontal distance beneath the landfill, and the phreatic surface represents a free boundary for the flow problem (Figure 8). Using the Dupuit-Forchheimer approximation, the saturated thickness, h, can be determined as a function of the values h_1 and h_2 measured at $x = 0$ and $x = \ell$, respectively:

$$h^2 = h_1^2 - \frac{h_1^2 - h_2^2}{\ell} x + \frac{a_d q}{k_{aq}} (\ell - x) x \tag{93}$$

where k_{aq} is the hydraulic conductivity of the aquifer.

The horizontal discharge can be expressed as follows:

$$Q_x = q_x h = \frac{k_{aq}}{2\ell} \left(h_1^2 - h_2^2 \right) - \frac{a_d q \ell}{2} + a_d q x \, . \tag{94}$$

The vertical groundwater velocity, q_z taken as positive in the upward direction, such as the z axis in Figure 8, can be derived from the following continuity equation of flow:

$$\frac{\partial q_x}{\partial x} + \frac{\partial q_z}{\partial z} = 0 \, . \tag{95}$$

Under unconfined conditions, h is not constant and equation (67) can be expressed as follows:

$$\frac{dh}{dx} q_x + h \frac{dq_x}{dx} = a_d q \, . \tag{96}$$

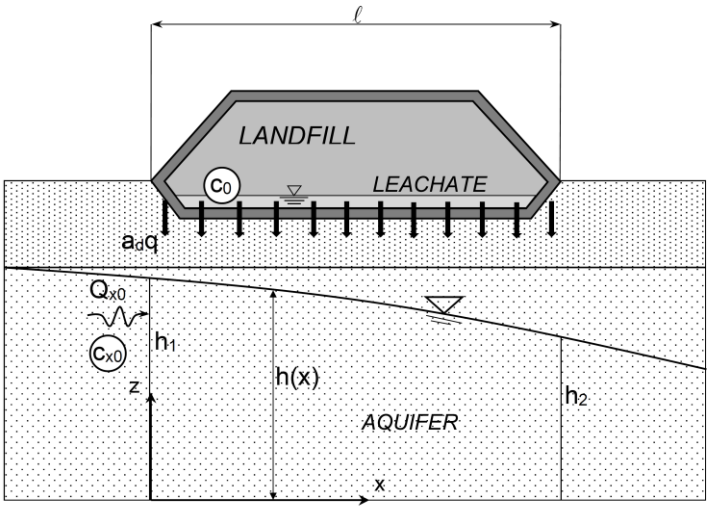


Figure 8. *Reference scheme for a thick aquifer beneath a landfill, under unconfined flow conditions. h(x) = saturated thickness of the aquifer, $h_1 = h(x = 0)$, $h_2 = h(x = \ell)$, q = vertical volumetric flux, c_0 source pollutant concentration, Q_{x0} = horizontal discharge upstream from the landfill, c_{x0} pollutant concentration upstream from the landfill.*

Using the continuity equation (95) and equation (96), q_z is found to be given by:

$$q_z = \frac{z}{h}\left(\frac{Q_x}{h}\frac{dh}{dx} - a_d q\right). \tag{97}$$

where the following boundary condition has been assumed: $q_z(z = 0) = 0$.

Using equations (93), (94) and (97), q_z can be calculated as a function of the space variables x and z in any point of the aquifer. The first term between the round brackets is due to the curving phreatic surface and was also found by Polubarinova-Kochina (1962) and Haitjema (1995). When h = constant and $dh/dx = 0$, q_z assumes the same expression that was found for confined flow conditions.

The pollutant mass balance can be expressed as follows under steady-state conditions:

$$q_x \frac{\partial c}{\partial x} = \alpha_T q_{x0} \frac{\partial^2 c}{\partial z^2} - q_z \frac{\partial c}{\partial z}\,. \tag{98}$$

The main difficulty in solving equation (98) is related to the presence of a free-boundary at $z = h$, where the following boundary condition must be imposed:

$$q_z c - \alpha_T q_{x0} \frac{\partial c}{\partial z} = -a_d q \frac{c_0 e^{P_L} - c}{e^{P_L} - 1} - (1 - a_d)\Lambda_d (c_0 - c)\,. \tag{99}$$

In order to solve such a problem, a possible strategy is to employ a coordinate transformation to map the domain onto a fixed region (Crank, 1987).

Passing from the coordinates (x,z) to the coordinates (χ,ζ) that are defined as follows:

$$\chi = x \tag{100}$$

$$\zeta = \frac{z}{h}, \tag{101}$$

the pollutant mass balance equation must be modified using the following rules of derivation:

$$\frac{\partial}{\partial \chi} = \frac{\partial}{\partial x} + \zeta \frac{dh}{d\chi}\frac{\partial}{\partial z}\,. \tag{102}$$

$$\frac{\partial}{\partial \zeta} = h \frac{\partial}{\partial z} \tag{103}$$

The pollutant mass balance becomes:

$$q_x\left(\frac{\partial c}{\partial \chi} - \frac{\zeta}{h}\frac{dh}{d\chi}\frac{\partial c}{\partial \zeta}\right) = \frac{\alpha_T q_{x0}}{h^2}\frac{\partial^2 c}{\partial \zeta^2} - \frac{q_z}{h}\frac{\partial c}{\partial \zeta}\,. \tag{104}$$

This last equation can be solved in a rectangular domain $(0,0) \times (\ell,1)$ with the following boundary conditions:

$$q_z c - \alpha_T q_{x0} \frac{\partial c}{\partial \zeta} = -a_d q \frac{c_0 e^{P_L} - c}{e^{P_L} - 1} - (1 - a_d)\Lambda_d (c_0 - c) \quad \text{at} \quad \zeta = 1 \tag{105}$$

$$q_z c - \alpha_T q_{x0} \frac{\partial c}{\partial \zeta} = 0 \quad \text{at} \quad \zeta = 0\,. \tag{106}$$

$$c = c_{x0} \quad \text{at } \chi = 0\,. \tag{107}$$

The condition given by equation (106) assumes that the pollutant flux is null at the bottom of the aquifer. A solution of equation (104), associated with the boundary conditions given by equations (105)-(107), can be obtained by a numerical method, such as that developed by Dominijanni and Manassero (2021).

5 APPLICATION EXAMPLES

The following examples are provided to illustrate how the previously derived steady-state solutions can be employed in order to assess the equivalency and the effectiveness of different landfill barriers. Because any realistic analysis should be based on specific data that have been measured by means of field and laboratory tests, the results of the following examples are only representative of the proposed analysis approach and should not be generalized to analogous barriers that are characterized by different parameter values and/or are exposed to different boundary conditions.

Two barriers are considered herein: the first one is a composite barrier comprising a 1.5 mm thick geomembrane liner (GML) and a 1 m thick compacted clay liner (CCL), which overlies a 3 m thick attenuation layer (AL); the second one is a composite barrier comprising a 1.5 mm thick geomembrane liner (GML) and a 10 mm thick geosynthetic clay liner (GCL), which overlies a 4 m thick attenuation layer (AL) (Figure 9). The two barriers are therefore characterized by approximately the same total thickness (i.e., $L \cong 4$ m).

The height of the ponded leachate in the drainage layer (also called leachate collection and removal system), h_p, is assumed equal to 0.5 m, which is the minimum thickness of the drainage layer that is required by European Directive 1999/31/EC (EC, 1999), and the hydraulic head at the bottom of the barrier, h_b, is assumed equal to 1.5 m. As a result, the difference in the hydraulic head between the top of the mineral layers and the bottom of the AL, $\Delta h = h_p + L - h_b$, equal to 3 m (Figure 9).

The physical, hydraulic and transport parameters that have been assigned to the geomembrane and the mineral layers are reported in Figure 9 and in Table 2. The CCL is hypothesized to be characterized by an average value of the hydraulic conductivity that corresponds to the maximum value that is admitted by the European and US regulations, that is $k = 1 \cdot 10^{-9}$ m/s. The porosity, n, and tortuosity factor, τ_m, values have been estimated from the data on the kaolinite specimens that were tested by Shackelford and Daniel (1991a,b). The GCL hydraulic conductivity and porosity values are derived from the results of the laboratory test conducted by Puma et al. (2015) with an aggressive permeant solution of 0.25 M of $CaCl_2$ under an effective confining stress of 70 kPa. These selected values take into account the increase in hydraulic conductivity and the reduction in void ratio that are induced by a long-term permeation with an aqueous solution with a high salt concentration. The GCL tortuosity factor is derived from the data on the sodium bentonite specimen tested by Dominijanni et al. (2013), neglecting the solute restriction effect that is related to chemico-osmotic phenomena. Typical parameter values of a silty soil have been selected for the AL (Manassero et al., 2000; Rowe and Brachman, 2004; Rowe et al., 2004).

Table 2. *Physical, hydraulic and transport parameters of the geomembrane and the mineral layers of the example landfill barriers.*

Parameter	**Mineral layers**		
	CCL	**GCL**	**AL**
Thickness, L (m)	1	0.01	3-4
Hydraulic conductivity, k (m/s)	$1 \cdot 10^{-9}$	$3.5 \cdot 10^{-10}$	$1 \cdot 10^{-7}$
Porosity (-)	0.55	0.69	0.3
Tortuosity factor, τ_m (-)	0.1	0.31	0.25
	Geomembrane		
Thickness, L_g (m)	0.0015		
Partition coefficient for toluene, K_g (-)	96		
Diffusion coefficient for toluene, D_g (m^2/s)	$0.47 \cdot 10^{-12}$		

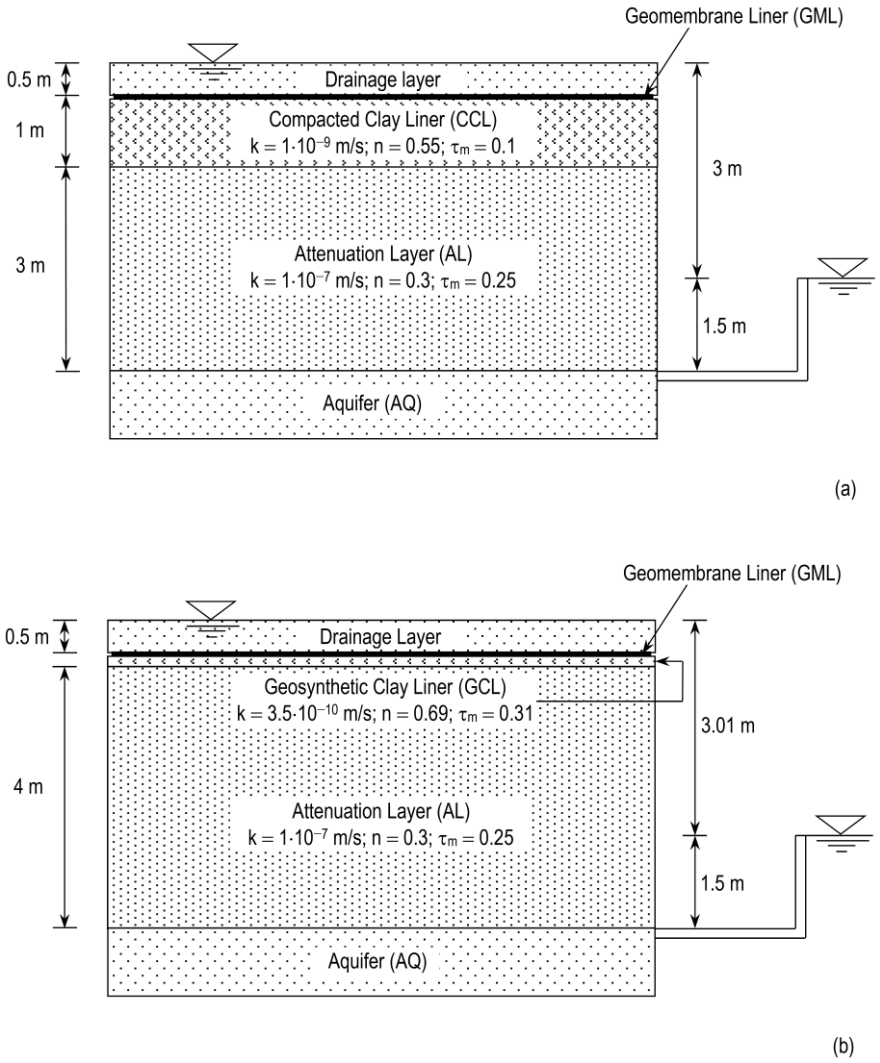


Figure 9. *Scheme of the two barriers considered in the example analysis: (a) composite barrier constituted by a geomembrane liner (GML) and a compacted clay liner (CCL); (b) composite barrier constituted by a GML and a geosynthetic clay liner (GCL).*

The analyses are developed for two contaminants: (1) cadmium (Cd) and (2) toluene (C_6H_5-CH_3), which are common components of municipal solid waste landfill leachates.

The leakage rate per unit area, q_d, has been calculated by using equation (27) and assuming: 1 hole in a wrinkle per hectare, $L_d = 3$ m, $2b = 0.2$ m, $\vartheta = 4 \cdot 10^{-8}$ m2/s for the contact between GML and CCL and $\vartheta = 3.5 \cdot 10^{-11}$ m^2/s for the contact between GML and GCL. The value of transmissivity, ϑ, that has been assigned to the GML - CCL contact represents the average value of the range estimated by Rowe (1998), which varies from $1.6 \cdot 10^{-8}$ m^2/s to $1 \cdot 10^{-7}$ m^2/s for this type of composite barrier. Analogously, the value of transmissivity, ϑ, that has been assigned to the GML - GCL contact represents the average value of the range provided by Harpur et al. (1993), which varies between $6 \cdot 10^{-12}$ m^2/s and $2 \cdot 10^{-10}$ m^2/s (Rowe and Brachman, 2004).

The obtained results (Table 3) show that the leakage rate through the composite barrier with GCL (q_d = 3.4 lphd) is appreciably lower than the leakage rate through the composite barrier with CCL (q_d = 9.8 lphd), because of the better contact conditions between the GML and GCL.

Table 3. *Calculated values of transport parameters for the example landfill barriers.*

Parameter	GML + CCL +AL	GML + GCL + AL
Volumetric flux, q (m/s)	$2.91 \cdot 10^{-9}$	$4.39 \cdot 10^{-8}$
Volumetric flux through composite barrier, q_d (m/s)	$1.14 \cdot 10^{-11}$ (9.8 lphd*)	$3.92 \cdot 10^{-12}$ (3.4 lphd*)
Equivalent area fraction, a_d (-)	0.39 %	0.009 %
Cadmium equivalent diffusivity, Λ (m/s)	$1.23 \cdot 10^{-11}$	$1.34 \cdot 10^{-11}$
Toluene equivalent diffusivity, Λ (m/s)	$1.67 \cdot 10^{-11}$	$1.82 \cdot 10^{-11}$
Cadmium Peclet number, P_L (-)	236	3268
Toluene Pecle number, P_L (-)	175	2416
Toluene equivalent diffusivity for geomembrane, Λ_d (m/s)	$1.67 \cdot 10^{-11}$	$1.82 \cdot 10^{-11}$

* lphd = litres per hectare per day

The CCL barrier is characterized by a value of $q = 2.91 \cdot 10^{-9}$ m/s, which is significantly lower than the value $q = 4.39 \cdot 10^{-8}$ m/s that has been found for the GCL barrier. This high value of the volumetric flux of the GCL barrier is related to the degradation of the hydraulic containment ability of GCL, due to the permeation of aggressive aqueous solutions, which has been considered in the selection of the value to assign to the GCL hydraulic conductivity. The Peclet number of the considered example mineral barriers are larger than 4, thus showing that, in the absence of the geomembrane, advection controls the contaminant migration processes.

The free-solution diffusion coefficient is equal to $7.17 \cdot 10^{-10}$ m^2/s for cadmium (Shackelford and Daniel, 1991a) and $9.7 \cdot 10^{-10}$ m^2/s for toluene (Yaws, 1995). The average values of the geomembrane partition coefficient and the diffusion coefficient have been assumed equal to $K_g = 96$ and $D_g = 0.47 \cdot 10^{-12}$ m^2/s, respectively (Rowe, 1998), on the basis of the data by Park and Nibras (1993) pertaining to the migration of toluene in aqueous solutions. The effective diffusion coefficient for the mineral layers has been calculated as the product of the apparent tortuosity factor, τ_m, and the free-solution diffusion coefficient (Shackelford and Daniel, 1991a). As a first approximation, the mechanical dispersivity has been neglected, and the hydrodynamic dispersion coefficient has been assumed equal to the effective diffusion coefficient. The calculated values of the equivalent diffusivity, Λ and Λ_d, and the Peclet number, P_L, are reported in Table 3. Because of the very low values of the equivalent fraction area, a_d, for the contaminant transport that occurs in correspondence of geomembrane defects (0.39% for GML + CCL and 0.009% for GML + GCL), the transport is controlled by diffusion in the case of toluene, similarly to what was found by Katsumi et al. (2001) and Foose (2010) for organic contaminants.

When the performance of a composite barrier is assessed, the finite service life of the geomembrane needs to be taken into account (Sangam and Rowe, 2002; Rowe, 2005). For example, Rowe (2006) pointed out that the service life of geomembranes is of the order of 15-50 years at temperatures of 50-60 °C. As a result, an analysis of the contaminant transport has been conducted by assuming $a_d = 1$ to assess the barrier performance after geomembrane degradation.

5.1 Thin aquifer

If the aquifer beneath the landfill with a length ℓ of 1,000 m is sufficiently thin ($h = 3$ m), the analytical solution given by equation (79) can be used to assess the variation of the contaminant concentration in the aquifer along the direction of the groundwater flow. The highest concentration value is found at $x = \ell$, where is located the point of compliance.

The values of η and the relative concentration at $x = \ell$, which have been calculated assuming that the horizontal groundwater volumetric flux just upstream from the landfill, q_{x0}, is equal to $1 \cdot 10^{-6}$ m/s (= 31.6 m/yr), are reported in Table 4 for all the considered example barriers.

The calculated relative concentrations in the aquifer are shown as a function of the horizontal distance below the landfill in Figures 10 and 11, for cadmium and toluene, respectively.

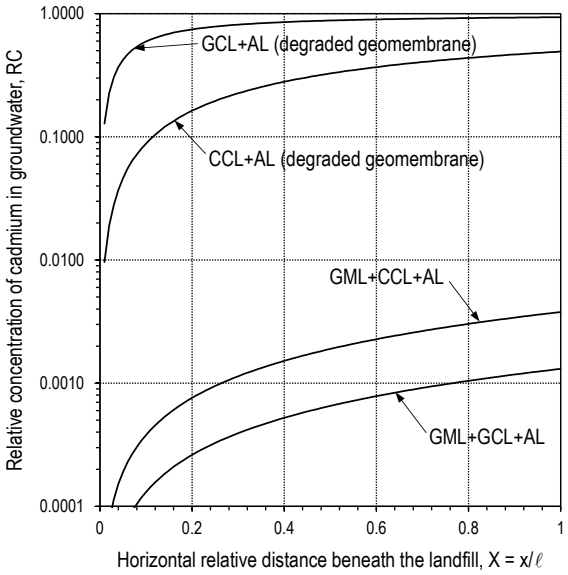


Figure 10. *Relative concentration of cadmium in a thin aquifer ($h = 3$ m, $q_{x0} = 1 \cdot 10^{-6}$ m/s) beneath the landfill ($\ell = 1000$ m).*

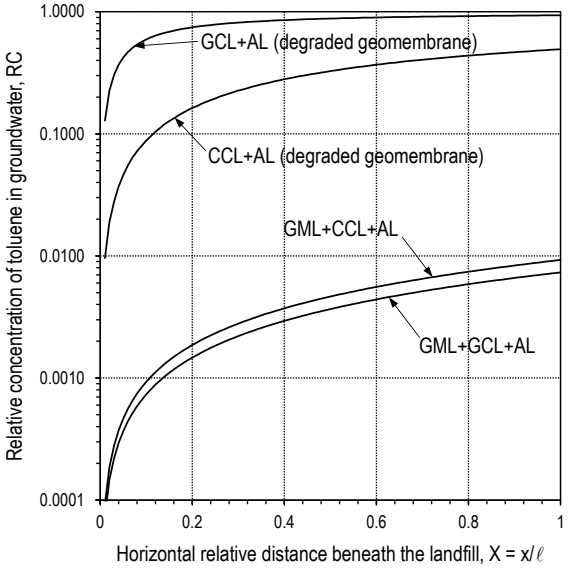


Figure 11. *Relative concentration of toluene in a thin aquifer ($h = 3$ m, $q_{x0} = 1 \cdot 10^{-6}$ m/s) beneath the landfill ($\ell = 1000$ m).*

The composite barrier with the GCL is more effective than the composite barrier with the CCL in reducing the toluene concentrations in the aquifer, even though a conservative value of the GCL hydraulic conductivity, which can be reached after a long-term permeation with an aggressive aqueous solution, has been assumed. The concentration of cadmium and toluene increases along the direction of the groundwater flow beneath the landfill. Therefore, the maximum value of contaminant concentration is reached at $x = \ell$, that is, just downstream from the landfill.

After the degradation of the geomembrane, the effectiveness of the barriers is reduced significantly and, as a result, the relative concentration below the landfill increases by more than one order of magnitude. Under such conditions, the CCL is more efficient than the GCL, due to the better ability of the CCL to reduce the contaminant diffusive flux.

5.2 Thick aquifer

If the aquifer thickness is not limited to a few meters, the vertical distribution of the contaminant needs to be taken into account by means of the analytical solutions or by means of the numerical solution (Dominijanni and Manassero, 2021). In this case, the contaminant concentration in the aquifer is not only dependent on the horizontal flushing that is determined by the groundwater flow, but also on the vertical dispersion. In this example, the aquifer thickness, h, has been assumed equal to 100 m and the transverse dispersivity within the aquifer, α_T, has been assumed equal to 1 m. The estimation of α_T was based on the indications of Rowe et al. (2004) in case of availability of high-quality experimental data.

The landfill length, ℓ, and the upstream horizontal groundwater volumetric flux, q_{x0}, have been assumed equal to 1000 m and $1 \cdot 10^{-6}$ m/s (= 31.6 m/yr), respectively, in the same way as for the thin aquifer example. The calculated relative concentrations of cadmium and toluene are shown in Figures 12 and 13, respectively, as a function of the aquifer depth, y, at the distances x = 100 m, 500 m and 1000 m (i.e., at X = 0.1, 0.5 and 1) beneath the landfill.

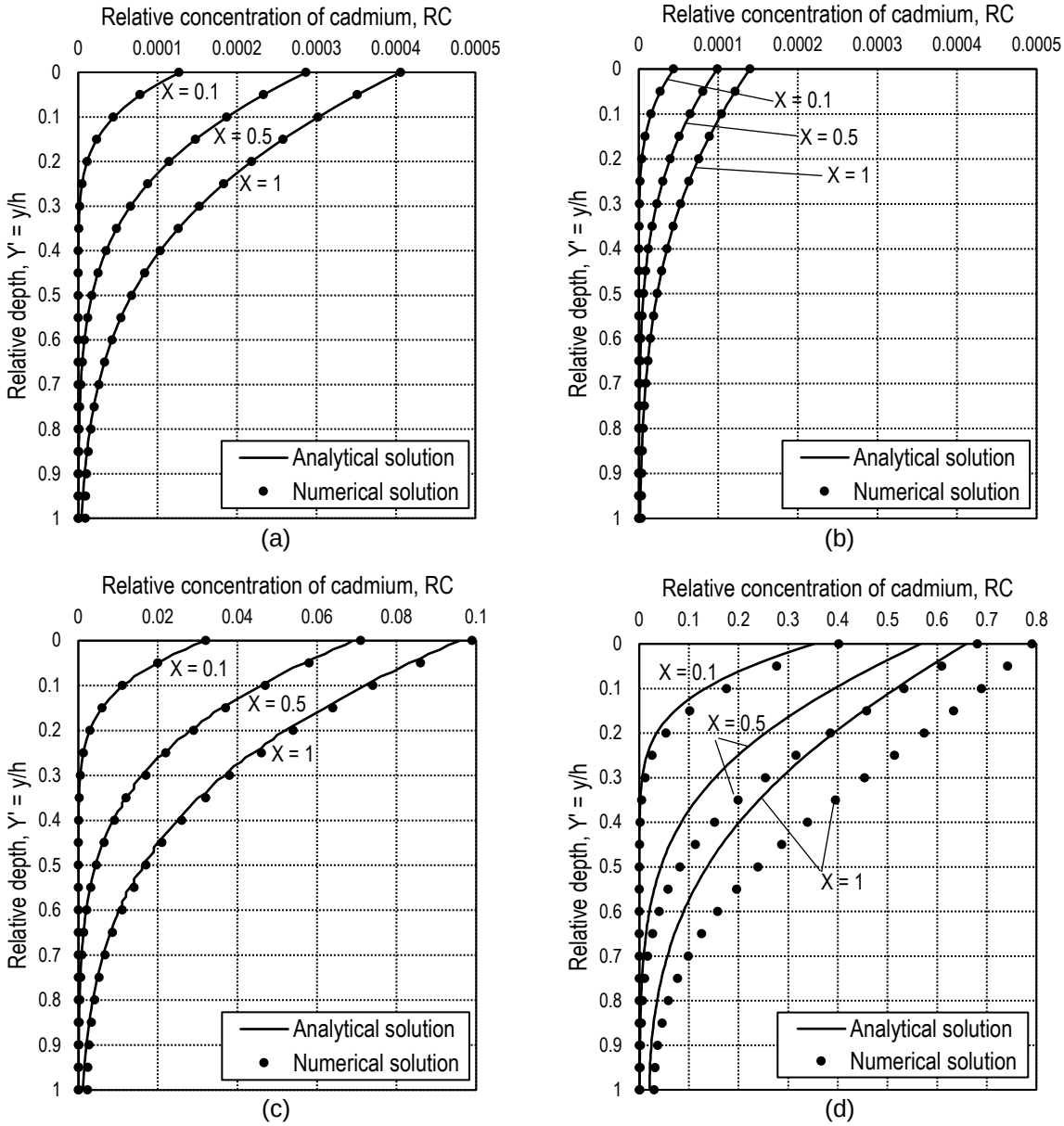


Figure 12. *Relative concentration of cadmium as a function of the relative depth, Y' = y/h, at X = 0.1, 0.5 and 1 for the following barriers: (a) GML + CCL + AL; (b) GML + GCL + AL; (c) CCL + AL (degraded geomembrane); (d) GCL + AL (degraded geomembrane).*

The contaminant concentration decreases with depth and increases over the horizontal distance. The relative concentration of toluene is higher than the relative concentration of cadmium due to the ability of the geomembrane to hinder the diffusion of inorganic contaminants, as already observed for the case of a thin aquifer.

The analytical solution for the barrier constituted by a GCL overlying an attenuation layer is not accurate, as the ratio $q/q_{x0} = 4.4\%$ is greater than 1% (Figure 12d and Figure 13d).

If a limiting value of the relative concentration is selected, a contaminant plume can be defined within the aquifer by means of the available analytical solution. For example, the toluene plumes corresponding to the limiting value of the relative concentration RC_{lim} of 0.01% are shown in Figure 14 for the two barrier examples with the intact geomembrane.

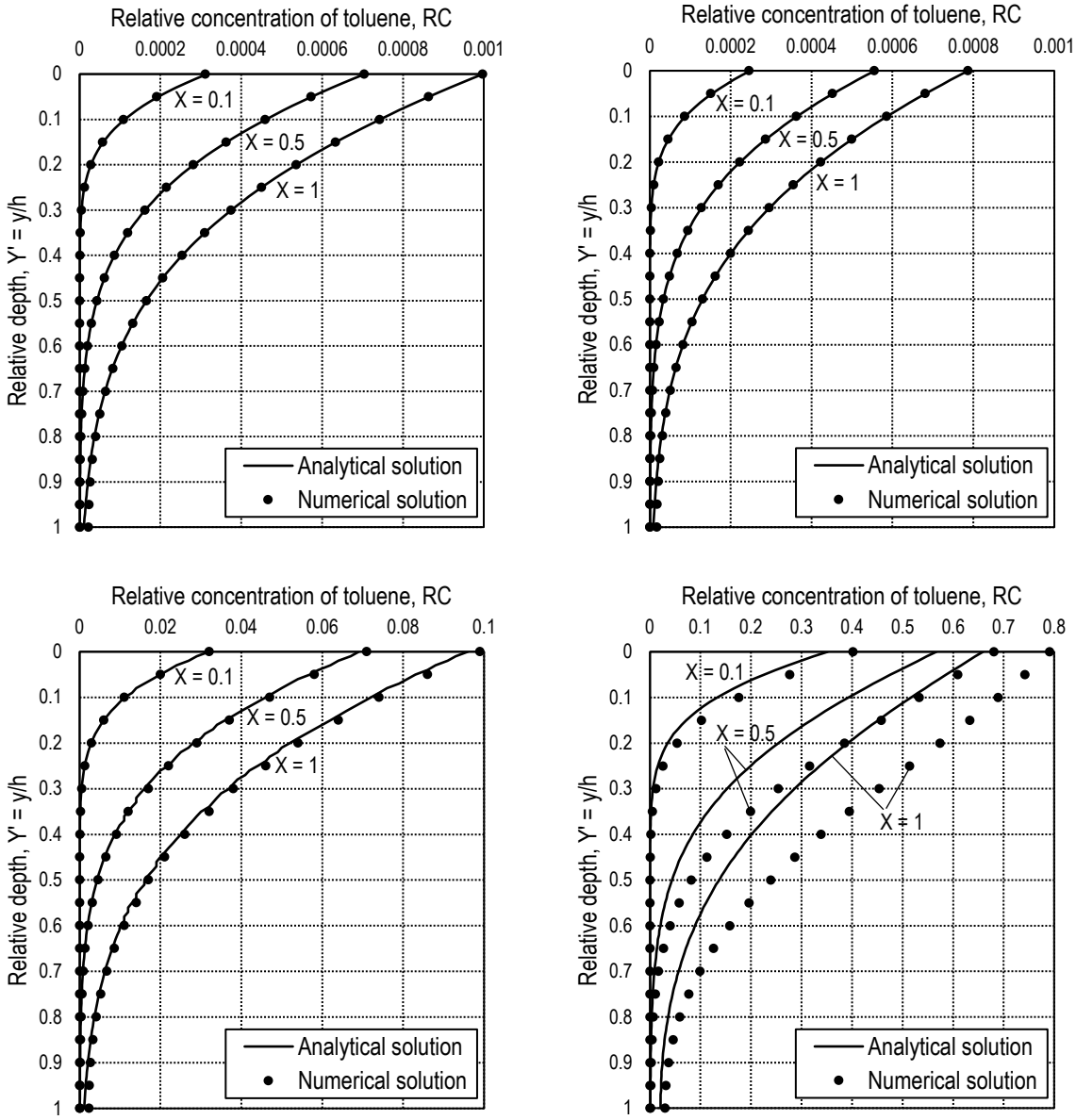


Figure 13. *Relative concentration of toluene as a function of the relative depth, Y' = y/h, at X = 0.1, 0.5 and 1 for the following barriers: (a) GML + CCL + AL; (b) GML + GCL + AL; (c) CCL + AL (degraded geomembrane); (d) GCL + AL (degraded geomembrane).*

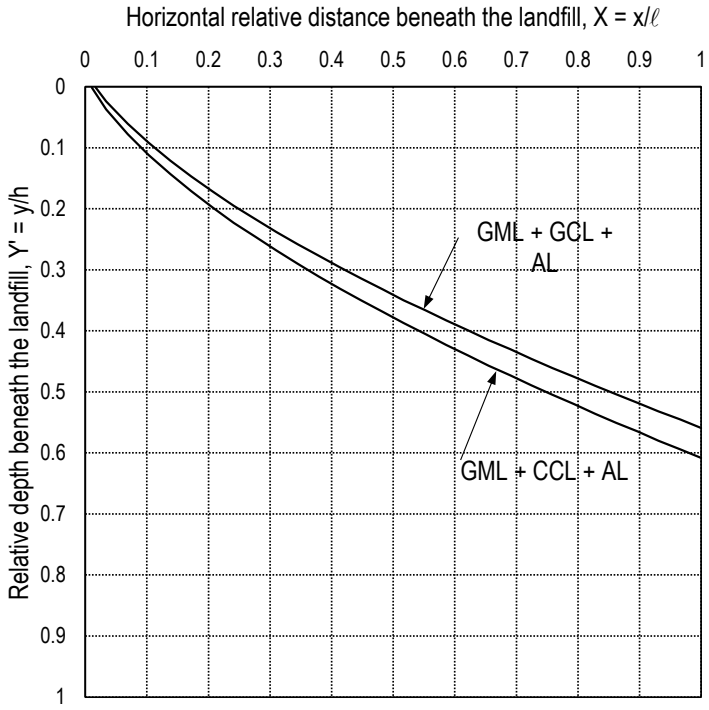


***Figure 14**. Toluene plume beneath the landfill for $RC_{lim} = 0.0001$ (0.01 %).*

6 CONCLUSIONS

The theoretical solutions described in this paper aim to model the contaminant transport from a source (e.g., contaminated soil or waste leachate) to the point of compliance located in the aquifer, downgradient from the landfill or the contaminated site. The calculated contaminant concentration must be less than a threshold value related to an unacceptable risk for human health through a toxicological model, which commonly considers vapour inhalation and groundwater ingestion as possible exposure paths.

The motivation for this theoretical work is supporting the transition from a prescriptive-based design approach to a performance-based design approach, in which the performance of the barrier system is demonstrated through theoretical analysis and not assumed *a priori*. A performance-based design is a fundamental requirement for sustainable landfilling and site remediation, as it allows the protection of the groundwater to be guaranteed while avoiding recourse to oversized barrier systems with relevant economic and environmental savings.

The mathematical solutions, which have been presented for the calculation of the contaminant concentration at the point of compliance, were derived under steady-state conditions, which exclude the possibility of modelling time-dependent phenomena, such as the reduction in time of a finite-mass source of contaminant or the contaminant concentration variations due to radioactive decay, biological degradation, sorption/desorption mechanisms and ion exchange.

The advantage of steady-state solutions is related to the widespread availability of data for the involved parameters and the relatively limited degree of uncertainty concerning such data. Moreover, these solutions allow for a conservative estimate of the contaminant concentration at the point of compliance. For these reasons, steady-state solutions are typically adopted in Tier-2 risk assessment analyses for contaminated sites and waste disposal facilities.

The solution presented in this paper are based on the following assumptions:

1) The source contaminant concentration is constant (i.e., the contaminant mass is infinite).
2) The transport through the barrier system is split into two contributions: an advective-diffusive flux that occurs through the geomembrane defects and a diffusive flux through the intact

geomembrane. The latter flux component is only of relevance for organic contaminants (i.e., VOCs) that are able to diffuse through polymeric sheets.

3) The contaminant flux through geomembrane defects is expressed as a one-dimensional flux that occurs through the mineral barrier underlying the geomembrane over an equivalent fraction of the total barrier area, a_d (≤ 1).
4) The equivalent fraction area for the contaminant transport is conservatively assumed to coincide with the equivalent fraction area for the volumetric or leakage flux through the geomembrane defects. The two equivalent fractions are expected to coincide when the contaminant transport is dominated by advection. Moreover, a formal theoretical correspondence can be found between the solution to the volumetric flux and the solution to the contaminant flux when pure diffusion occurs under perfect contact conditions between the geomembrane and the underlying mineral barrier. In the other cases, the equivalent fraction area for the contaminant transport is expected to be less than the equivalent fraction area for the volumetric flux.
5) The vertical contaminant flux through the barrier system is expressed through an analytical solution, which can be introduced in the contaminant mass balance at the boundary with the adjacent aquifer.
6) The contaminant concentration in the aquifer can be obtained from a finite-difference numerical solution in the most general case. However, analytical solutions are available for the following cases: (a) thin aquifers beneath a landfill; (b) semi-infinite or finite aquifers beneath a landfill or alongside a cutoff wall when the groundwater velocity in the vertical direction is less than 1% of groundwater velocity in the horizontal direction.

The proposed method is flexible and can be applied using different theoretical methods to calculate the volumetric flux through the mineral barrier, q, and the equivalent area fraction for the contaminant transport through the geomembrane defects, a_d. For instance, numerical solutions can be used to evaluate the volumetric flux, q, taking into account the condition of partial saturation that may occur in the attenuation natural layers of the barrier system. The equivalent area fraction, a_d, can be estimated through several theoretical or empirical equations derived for the calculation of the leakage rate, considering defects of different sizes and shapes. If the geomembrane is absent or so degraded that has lost its barrier ability, a_d is taken equal to 1.

The analysis can be extended to time-dependent problems using a single-step application of the Domain Decomposition Method described in the Introduction. As shown in Figure 15, the contaminant transport through the barrier system of a landfill can be calculated through a finite-difference one-dimensional model by imposing a known concentration at the top boundary to represent the contaminant source and a null concentration at the bottom boundary. The latter condition allows for maximising the contaminant flux, $J_s(t)$, exiting from the barrier system and entering the underlying aquifer. The analysis is split into two parts to account for the advective-diffusive transport through the defects of the geomembrane and the pure diffusive transport of organic contaminants through the intact geomembrane. The calculated contaminant flux, $J_s(t)$, exiting from the barrier system is imposed as a top boundary condition for the problem related to the contaminant transport in the aquifer. In the most general case of a thick aquifer, the analysis is conducted using a finite-difference two-dimensional model, which allows calculating the distribution of the contaminant concentration within the aquifer as a function of time, $c(x,y,t)$.

The proposed numerical procedure allows non-linear sorption phenomena and spatial changes in the transport properties of the barrier system to be taken into account. As a result, the method is appropriate for most of the expected field scenarios while maintaining an acceptable simplicity of implementation.

However, the possibility of successfully applying the procedure is strictly dependent on the availability of reliable values for the involved parameters and a correct representation of the field boundary conditions.

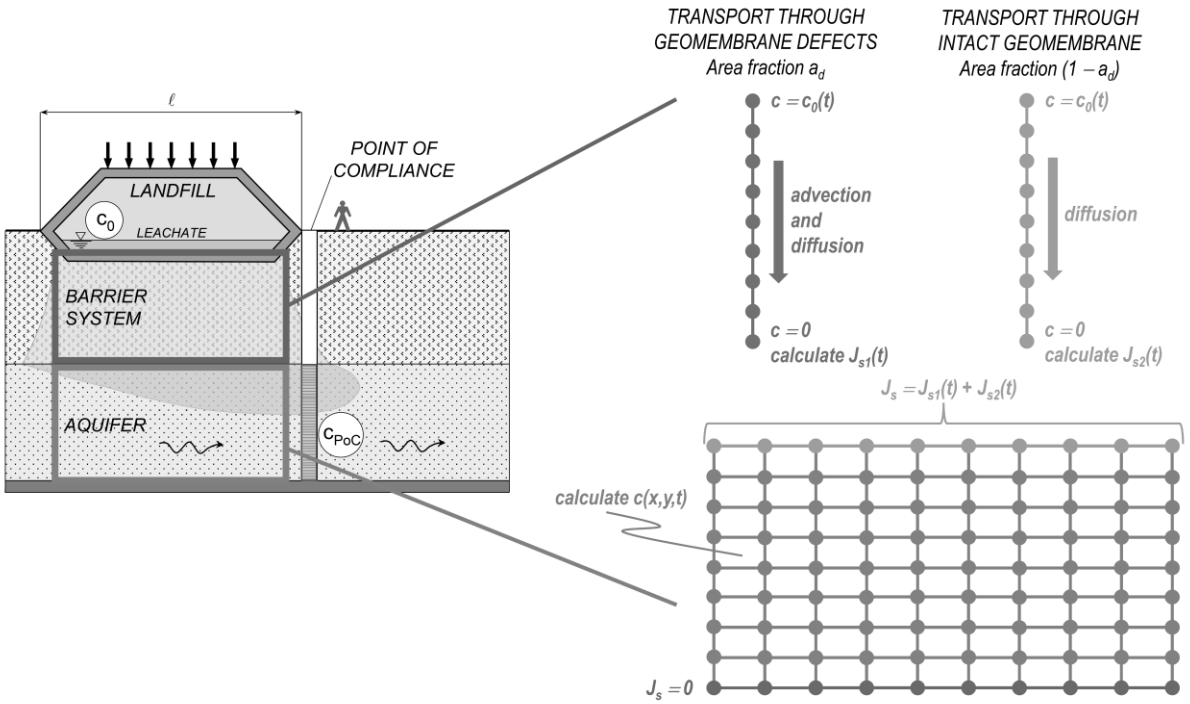


***Figure 15**. Application of the proposed approach to a time-dependent analysis of contaminant migration from a landfill to a point of compliance, which is located in the aquifer beneath the landfill.*

REFERENCES

ASTM (1995). E1739 – 95. Standard guide for risk-based corrective action applied at petroleum release sites, Technical report, West Conshohocken, PA.

ASTM (2000). E2081 – 00. Standard guide for risk-based corrective action, Technical report, West Conshohocken, PA.

Bear, J. (1972). Dynamics of Fluids in Porous Media. New York: Elsevier.

Bellomo, N., and Preziosi, L. (1995). Modelling Mathematical Methods and Scientific Computation, CRC Press.

Carslaw, H.S., and Jaeger, J.C. (1959). Conduction of heat in solids. Oxford: Clarendon Press.

Charbeneau, R.J. (2000). Groundwater hydraulics and pollutant transport. Upper Saddle River, New Jersey: Prentice Hall.

Crank, J. (1975). The mathematics of diffusion, Second Edition. Oxford: Clarendon Press.

Crank, J. (1987). Free and Moving Boundary Problems. Oxford: Clarendon Press.

Dachler, R. (1936). Grundwasserströmung, Wien: Springer.

Dominijanni, A. and Manassero, M. (2021). Steady-state analysis of pollutant transport to assess landfill liner performance. Environmental Geotechnics, 8(7), 480-494.

Dominijanni, A., Guarena, N. and Manassero, M. (2021a). Risk assessment procedure for the performance-based design of landfill lining systems and cutoff walls. Japanese Geotechnical Society Special Publication, Vol. 9(5), 2021, Third International Symposium on Coupled Phenomena in Environmental Geotechnics, Kyoto, Japan, 20-21 October 2021, 199-204.

Dominijanni, A., Guarena, N. and Manassero, M. (2021b). La progettazione prestazionale dei sistemi di contenimento degli inquinanti nelle discariche. In Moraci, N., and Soccodato, C. (Eds.), Atti del XXVII Convegno Nazionale di Geotecnica, La Geotecnica per lo Sviluppo Sostenibile del Territorio e per la Tutela dell'Ambiente, 13-15 Luglio 2022, Reggio Calabria, Roma: Associazione Geotecnica Italiana (AGI), Vol. 1, pp. 79-124.

Dominijanni, A., Manassero, M. and Puma, S. (2013). Coupled chemical-hydraulic-mechanical behaviour of bentonites. Géotechnique, 63(3), 191-205.

Estrin, D., and Rowe, R.K. (1995). Landfill design and the regulatory system. Proceedings of the 5th International Landfill Symposium, Sardinia, Italy, Vol. 3, 15-26.

Foose, G.J. (2010). A steady-state approach for evaluating the impact of solute transport through composite liners on groundwater quality. Waste Management, 30(8–9), 1577-1586.

Foose, G.J., Benson, C.H., and Edil, T.B. (2001). Predicting leakage through composite landfill liners. Journal of Geotechnical and Geoenvironmental Engineering,127(6), 510-520.

Forchheimer, P. (1930). Hydraulik, Third Edition, Leipzing und Berlin: B.G. Teubner.

Gardner, W.R. (1958). Steady state solutions of the unsaturated moisture flow equation with application to evaporation from a water table. Soil Science, 85, 228-232.

Giroud, J.P. (1997). Equations for calculating the rate of liquid migration through composite liners due to geomembrane defects. Geosynthetics International, 4(3-4), 335-348.

Giroud, J.P. (2016). The fifth Victor De Mello Lecture. Leakage control using geomembrane liners, Soils and Rocks, 39(3), 213-235.

Giroud, J.P., and Bonaparte, R. (1989). Leakage through liners constructed with geomembrane liners-parts I and II and technical note. Geotextiles and Geomembranes, 8(1), 27-67, 8(2), 71-111, 8(4), 337-340.

Giroud, J.P., Badu-Tweneboah, K., and Soderman, K.L. (1997). Comparison of leachate flow through compacted clay liners and geosynthetic clay liners in landfill liner systems. Geosynthetics International, 4(3-4), 391-431.

Guarena, N., Dominijanni, A., and Manassero, M. (2020). From the design of bottom landfill liner systems to the impact assessment of contaminants on underlying aquifers. Innovative Infrastructure Solutions, 5, 2.

Guyonnet, D., Perrochet, P., Côme, B., Seguin, J.-J. and Parriaux, A. (2001). On the hydro-dispersive equivalence between multi-layered mineral barriers. Journal of Contaminant Hydrology, 51(3-4), 215-231.

Haitjema, H.M. (1995). Analytic element modeling of ground-water flow. San Diego: Academic Press.

Harr, M.E. (1962). Groundwater and Seepage. New York: McGraw-Hill.

ISPRA (2011). Nota integrativa della nota ISPRA prot. N. 30237 del 16/09/2010 sull'applicazione della circolare del Ministero dell'Ambiente e della Tutela del Territorio e del Mare n. 0014963 del 30/06/2009. Prot. ISPRA n. 36365 del 31/10/2011.

Jonas, H. (1979). Das Prinzip Verantwortung: Versuch einer Ethik für die technologische Zivilisation. Frankfurt am Main: Insel-Verlag. English translation: Jonas, H. (1984). The Imperative of Responsibility: In Search of Ethics for the Technological Age. Chicago: The University of Chicago Press.

Katsumi, T., Benson, C.H., Foose, G.J. and Kamon, M. (2001). Performance-based design of landfill liners. Engineering Geology, 60(1-4), 139-148.

Lu, N., and Griffiths, D.V. (2004). Profiles of Steady-State Suction Stress in Unsaturated Soils. Journal of Geotechnical and Geoenvironmental Engineering, 130(10), 1063-1076.

Lu, N., and Likos, W.J. (2004). Unsaturated soil mechanics. Hoboken, New Jersey: Wiley.

Manassero, M., Benson, C.H., and Bouazza, A. (2000). Solid waste containment systems, Proceedings of GeoEng2000, Vol. 1, Technomic, Lancaster, PA, 520-642.

Manassero, M., Fratalocchi, E., Pasqualini, E., Spanna, C., and Verga, F. (1995). Containment with Vertical Cutoff Walls.In: Acar, Y.B., and Daniel, D.E. (Eds.), Geoenvironment 2000, Vol. 2, Characterization, Containment, Remediation, and Performance in Environmental Geotechnics, Geotechnical Special Publication No. 46, New York: ASCE, pp. 1142-1172.

Park, J.K. and Nibras, M. (1993). Mass flux of organic chemicals through polyethylene geomembranes. Water Environment Research, 65(3), 227-237.

Philip, J.R. (1968). Steady infiltration from buried point sources and spherical cavities. Water Resources Research, 4(5), 1039-1047.

Polubarinova-Kochina, P.Y. (1962). Theory of ground water movement. Princeton: Princeton University Press.

Puma, S., Dominijanni, A., Manassero, M. and Zaninetta, L. (2015). The role of physical pretreatments on the hydraulic conductivity of natural sodium bentonites. Geotextiles and Geomembranes, 43(3), 263-271.

Raats, P.A.C. (1970). Steady infiltration from line sources and furrows. Soil Science Society of America Proceedings, 34(5), 709-714.

Rabideau, A., and Khandelwal, A. (1998). Boundary conditions for modeling transport in vertical barriers. Journal of Environmental Engineering, 124(11), 1135-1139.

Rowe, R. K. (1998). Geosynthetics and the minimization of contaminant migration through barrier systems beneath solid waste. Proceedings of the 6th International Conference on Geosynthetics, Atlanta, Industrial Fabrics Association International, St Paul, USA, 27-103.

Rowe, R.K. (2005). Long-term performance of contaminant barrier systems. 45th Rankine Lecture. Géotechnique, 55(9), 631-678.

Rowe, R.K. (2006). Some factors affecting geosynthetics used for geoenvironmental applications. In: Thomas, H.R. (Ed.), Proceedings of the 5th International Congress on Environmental Geotechnics, vol. 1. London: Thomas Telford, pp. 43-69.

Rowe, R.K. and Brachman, R.W.I. (2004). Assessment of equivalency of composite liners. Geosynthetics International, 11(4), 273-286.

Rowe, R.K., and Booker, J.R. (1985a). 1-D pollutant migration in soils of finite depth. Journal of Geotechnical Engineering, 111(4), 479-499.

Rowe, R.K., and Booker, J.R. (1985b). Two-dimensional pollutant migration in soils of finite depth. Canadian Geotechnical Journal, 22(4), 429-436.

Rowe, R.K., and Booker, J.R. (2005). POLLUTEv7: Pollutant migration through a nonhomogeneous soil, © 1983–2005. Distributed by GAEA Environmental Engineering Ltd, 87 Garden Street, Whitby, Ontario, Canada L1N 9E7.

Rowe, R.K., and Yu, Y. (2018). Tensile strains in geomembrane landfill liners. Keynote Lecture GeoShanghai 2018, In: Li, L., et al. (Eds.), GSIC 2018, Proceedings of GeoShanghai 2018 International Conference: Ground Improvement and Geosynthetics, pp. 1-10.

Rowe, R.K., Quigley, R.M., Brachman, R.W.I., and Booker, J.R. (2004). Barrier systems for waste disposal, Second Edition. London and New York: Spon Press.

Rubin, H. and Buddemeier, R.W. (1996). A top specified boundary layer (TSBL) approximation approach for the simulation of groundwater contamination processes. Journal of Contaminant Hydrology, 22(1-2), 123-144.

Sangam, H.P., and Rowe, R.K. (2002). Effects of exposure conditions on the depletion of antioxidants from high-density polyethylene (HDPE) geomembranes. Canadian Geotechnical Journal, 39(6), 1221-1230.

Sethi, R., and Di Molfetta, A. (2019). Groundwater Engineering. A Technical Approach to Hydrogeology, Contaminant Transport and Groundwater Remediation, Springer.

Shackelford, C.D. (1990). Transit-time design of earthen barriers. Engineering Geology, 29(1), 79-94.

Shackelford, C.D. (1993). Contaminant transport. Chapter 3. In: Daniel, D.E. (Ed.), Geotechnical practice for waste disposal. London: Chapman and Hall, pp. 33-65.

Shackelford, C.D. (2014). The ISSMGE Kerry Rowe Lecture: The role of diffusion in environmental geotechnics. Canadian Geotechnical Journal, 51(11), 1219-1242.

Shackelford, C.D. and Daniel, D.E. (1991a). Diffusion in saturated soil: I. Background. Journal of Geotechnical Engineering, 117(3), 467-484.

Shackelford, C.D. and Daniel, D.E. (1991b). Diffusion in saturated soil: II. Results for compacted clay. Journal of Geotechnical Engineering, 117(3), 485-506.

Shackelford, C.D. and Rowe R.K. (1998). Contaminant transport modeling. In: Sêco e Pinto, P.S. (Ed.), Proceedings of the 3rd International Congress on Environmental Geotechnics. Rotterdam: Balkema, pp. 939-956.

US EPA (1989). Risk assessment guidance for superfund (RAGS): part A. Office of Emergency and Remedial Response, U.S. Environmental Protection Agency, Washington, D.C., USA.

Yaws, C.L. (1995). Handbook of transport property data. Houston: Gulf.